Particles and the Cosmos

2020/2021

Sascha Caron, Jörg Hörandel

NM109
first semester, 6 ec

28 hrs lecture	Tuesday	8:30 - 10:15
28 hrs problem session	Wednesday	10:30 - 12:15

Lectures:

Experimental methods (JRH)

01.09.2020 1. Interactions with matter
08.09.2020 2. Detectors

Standard model (SC)

15.09.2020 3. Particles, QED, Feynman rules
22.09.2020 4. Hadrons and QCD
29.09.2020 5. Hadrons and QCD
06.10.2020 6. Weak interactions, CP violation
13.10.2020 7. Higgs mechanism

Astroparticle physics (JRH)

03.11.2020 8. The birth of cosmic rays
10.11.2020 9. Cosmic rays in the Galaxy, in the heliosphere, and the Earth magnetic field
17.11.2020 10. Cosmic rays at the top of and in the atmosphere
24.11.2020 11. Cosmic rays underground - neutrino oscillations
01.12.2020 12. Neutrino oscillations

Beyond the Standard Model, Dark Matter (SC)

08.12.2020 13. Lambda CDM, Big-bang nucleosynthesis
15.12.2020 14. Dark matter - Beyond-the-standard-model reasons

for Astroparticle Physics

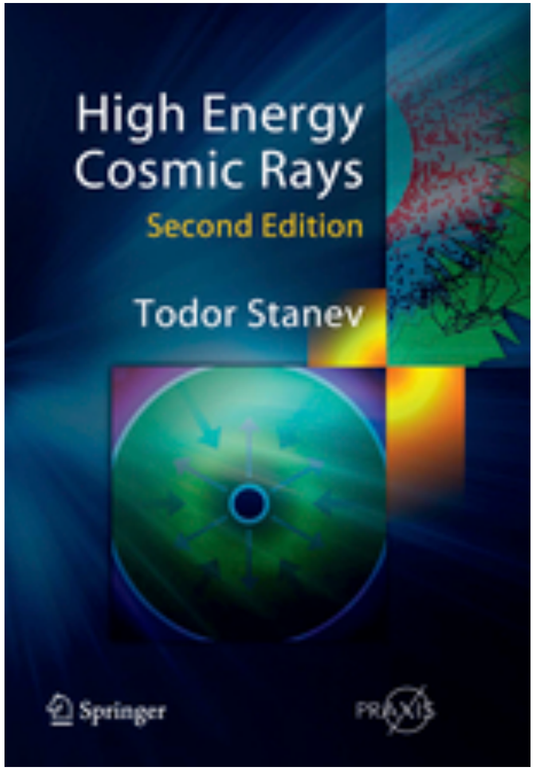

Jörg R. Hörandel
HG 02.728
http://particle.astro.ru.nl

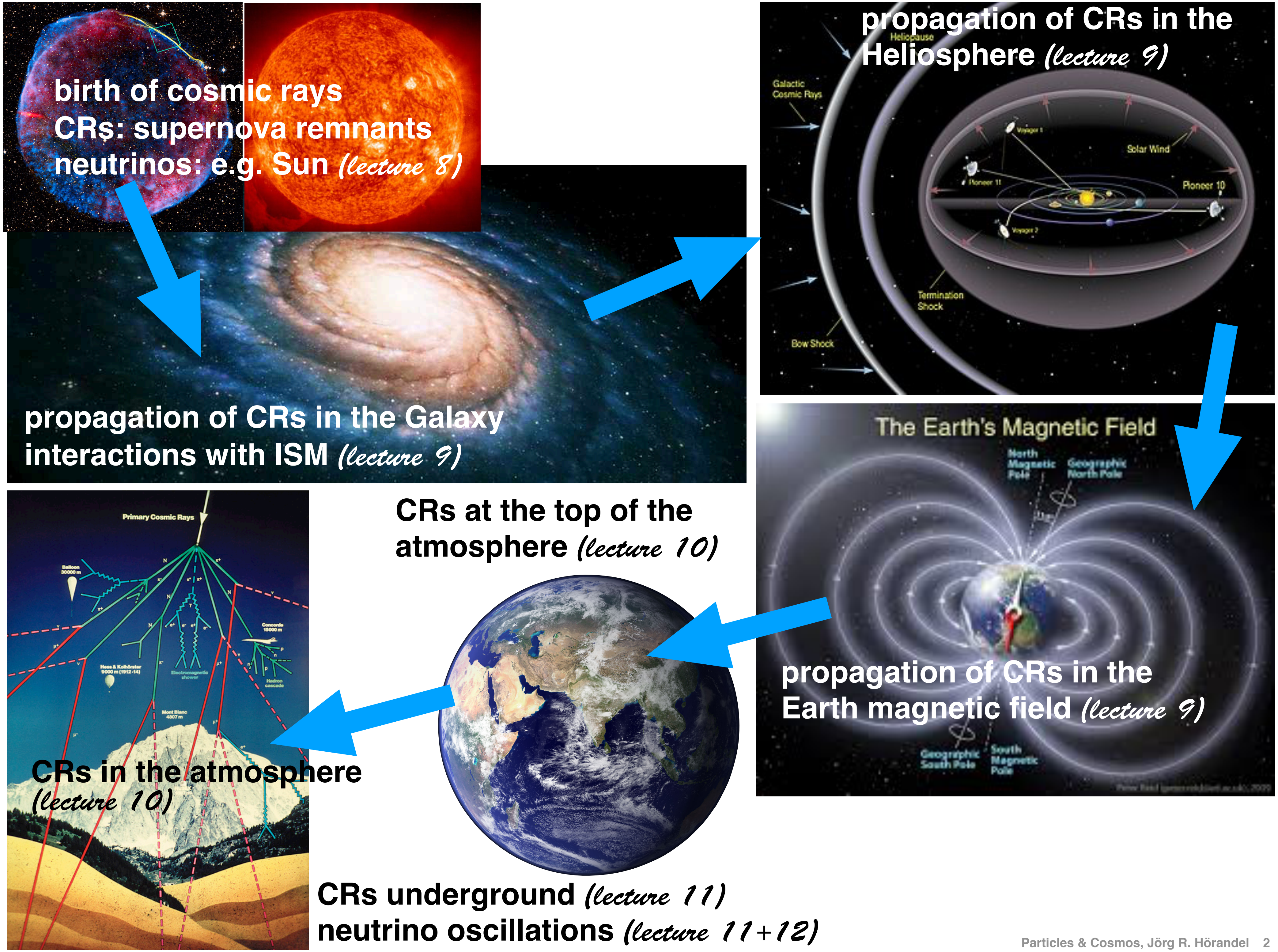

birth of cosmic rays
CRs: supernova remnants
neutrinos: e.g. Sun (lecture 8)
propagation of CRs in the Galaxy
interactions with ISM (lecture 9)
propagation of CRs in the
Heliosphere (lecture 9)
Heliopause
Galactic Cosmic Rays
Voyager 1
Solar Wind
Pioneer 11
Pioneer 10
Voyager 2
Termination Shock
Bow Shock
The Earth's Magnetic Field
North Magnetic Pole
Geographic North Pole
Geographic South Pole
South Magnetic Pole
propagation of CRs in the
Earth magnetic field (lecture 9)
CRs at the top of the
atmosphere (lecture 10)
Primary Cosmic Rays
CRs in the atmosphere
(lecture 10)
CRs underground (lecture 11)
neutrino oscillations (lecture 11+12)

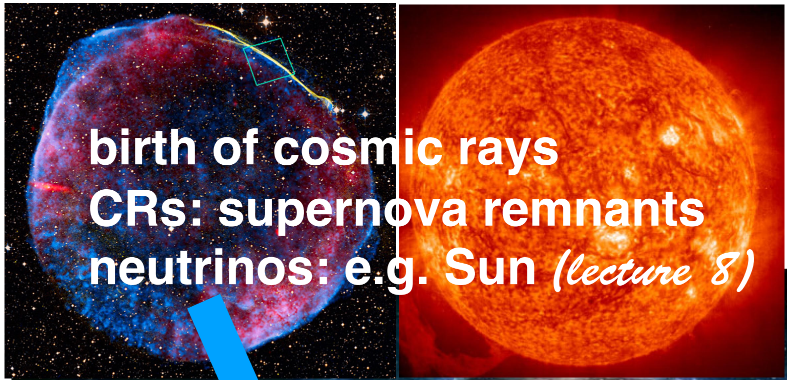

birth of cosmic rays
CRs: supernova remnants
neutrinos: e.g. Sun *(lecture 8)*

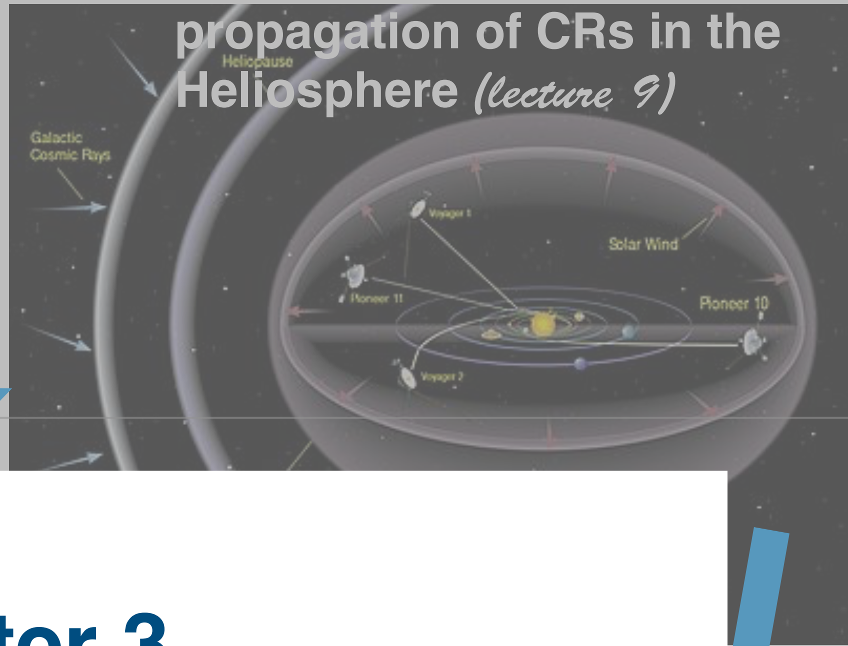

propagation of CRs in the
Heliosphere *(lecture 9)*

propagation of CRs in the
interactions with ISM *(lect*

today:
Stanev, chapter 3

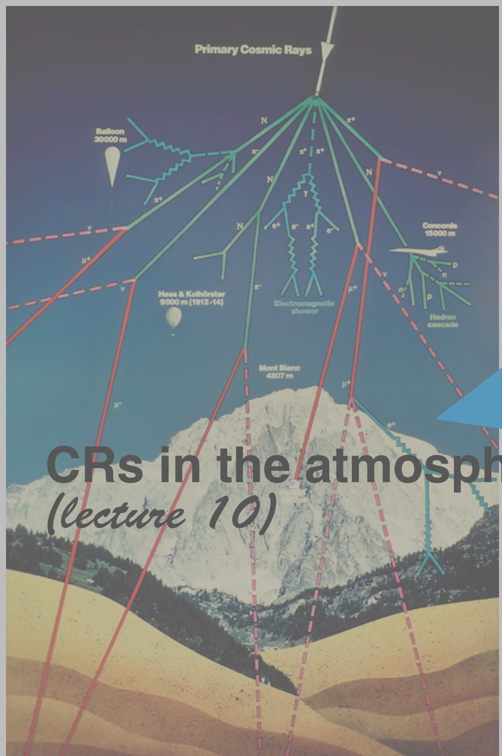

CRs in the atmosphere
(lecture 10)

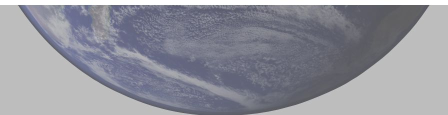

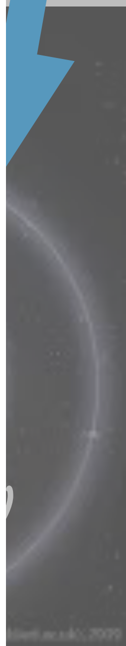

CRs underground *(lecture 11)*
neutrino oscillations *(lecture 11+12)*

The birth of cosmic rays

Stanev chapter 3

Stellar energetics. The pp chain

$$\frac{dP(r)}{dr} = -\frac{GM(r)\rho(r)}{r^2},$$

hydrostatic equilibrium in stars

P **pressure, dominated by thermal motion of electrons and ions** $\propto T^4$

stars radiate energy at high rate

$$\frac{dL_r}{dr} = 4\pi r^2 \times \rho \times \left(\varepsilon_{nucl} - T\frac{dS}{dt}\right),$$

rate at which energy is generated on the shell at distance *r* from the center

nuclear energy

rate of generation of mechanical energy through the stellar entropy *S* and the temperature *T*

for stars like the Sun on the main sequence of stellar evolution, nuclear energy dominates

$$t_{gravity} = G_N M_\odot^2 / R_\odot L_\odot \simeq 10^7 \text{ years.}$$

time scale for mechanical energy

$$t_{nucl} = \epsilon \times M_\odot c^2 / L_\odot \simeq 10^{10} \text{ years}$$

time scale for nuclear energy

Nuclear fusion

fusion of 4 protons to He nucleus
—> 24.7 MeV energy gain

p-p chain

1a	$\mathrm{p} + \mathrm{p}$	$\longrightarrow$	$^{2}\mathrm{H} + \mathrm{e}^{+} + \nu_e$
1b	$\mathrm{p} + \mathrm{e}^{-} + \mathrm{p}$	$\longrightarrow$	$^{2}\mathrm{H} + \nu_e$
2	$^{2}\mathrm{H} + \mathrm{p}$	$\longrightarrow$	$^{3}\mathrm{He} + \gamma$
3a	$^{3}\mathrm{He} + {}^{3}\mathrm{He}$	$\longrightarrow$	$^{4}\mathrm{He} + 2\ \mathrm{p}$
3b	$^{3}\mathrm{He} + {}^{4}\mathrm{He}$	$\longrightarrow$	$^{7}\mathrm{Be} + \gamma$
3c	$^{3}\mathrm{He} + \mathrm{p}$	$\longrightarrow$	$^{4}\mathrm{He} + \mathrm{e}+ + \nu_e$
4a	$^{7}\mathrm{Be} + \mathrm{p}$	$\longrightarrow$	$^{7}\mathrm{Li} + \nu_e$
4b	$^{7}\mathrm{Be} + \mathrm{p}$	$\longrightarrow$	$^{8}\mathrm{B} + \gamma$
5a	$^{7}\mathrm{Li} + \mathrm{p}$	$\longrightarrow$	$2 \times {}^{4}\mathrm{He}$
5b	$^{8}\mathrm{B}$	$\longrightarrow$	$^{8}\mathrm{B}^{*} + \mathrm{e}^{+} + \nu_e$
6b	$^{8}\mathrm{B}^{*}$	$\longrightarrow$	$2 \times {}^{4}\mathrm{He}$

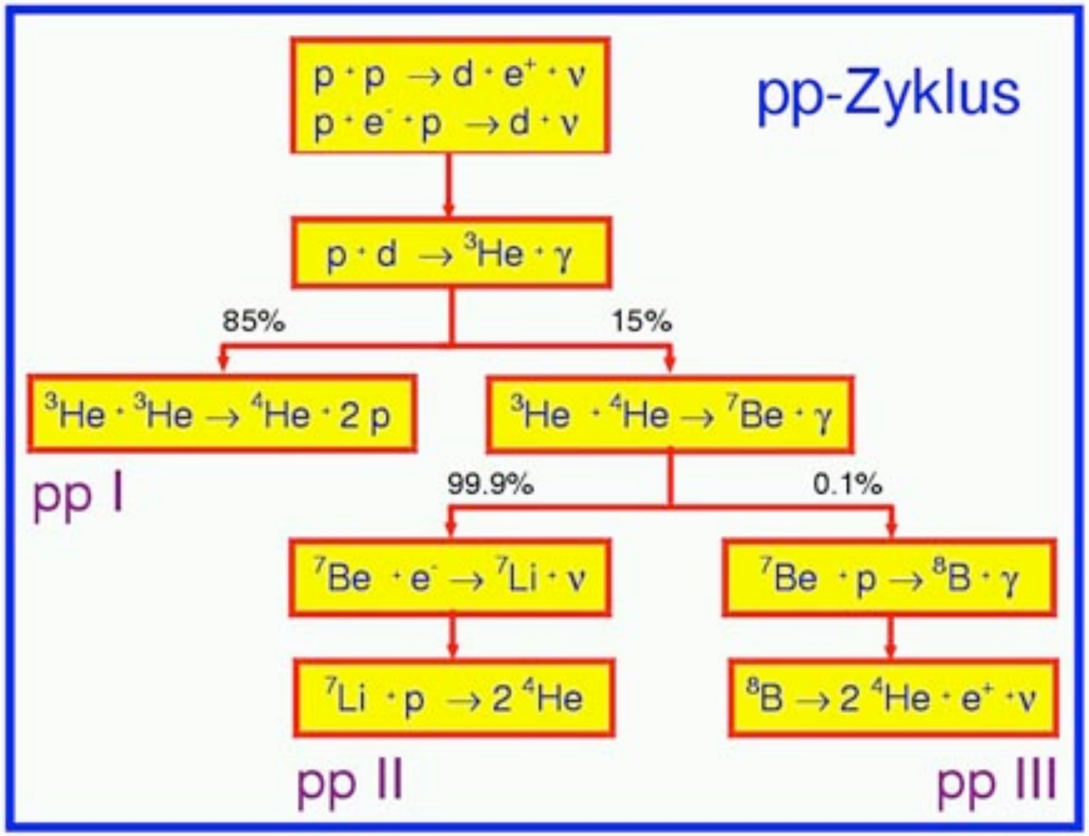

Neutrinos from the Sun - Hydrogen burning

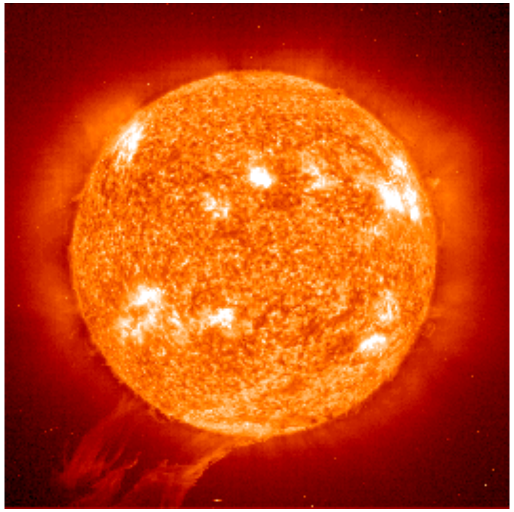

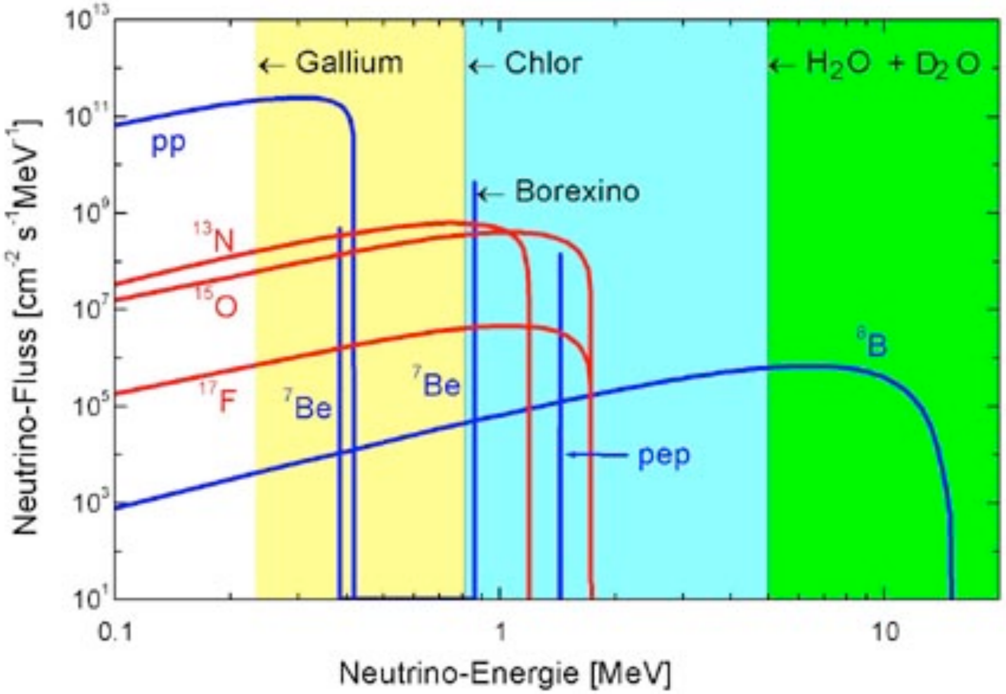

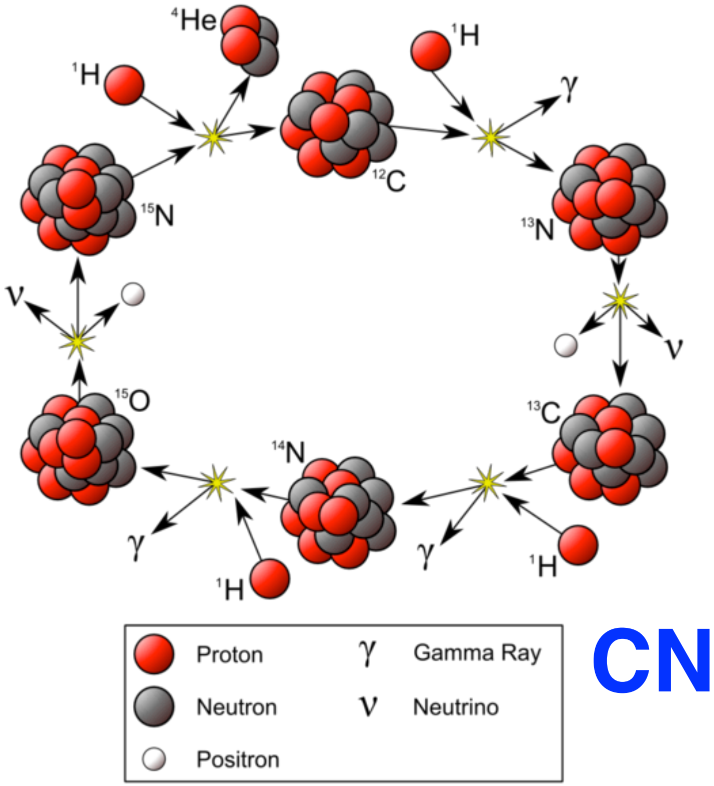

CNO cycle

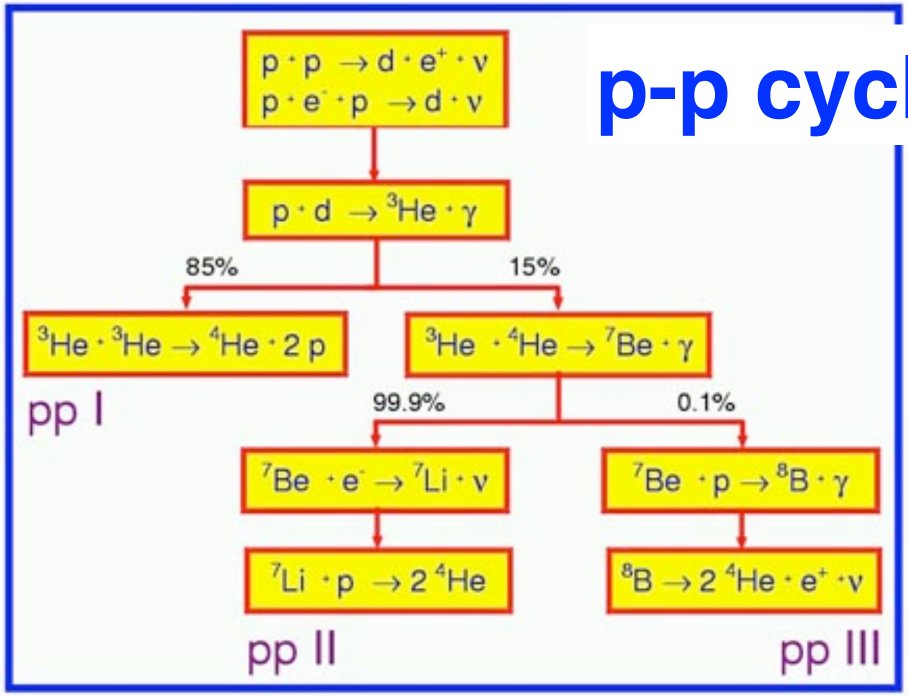

p-p cycle

Solar neutrinos

solar luminosity $L_{\odot}/10\ \mathrm{MeV} \simeq 10^{38}$ per second.

neutrino flux at Earth (distance 1 AU to Sun) $F_{\nu} \simeq 2.5 \times 10^{38}/4\pi d^2 \simeq 10^{11}\ \mathrm{cm}^{-2}\mathrm{s}^{-1}$

two principal methods to detect neutrinos:

- **radiochemical method, using inverse beta decay**
- **neutrino (electron) scattering**

the methods have different energy thresholds

neutrino cross sections are small
—> difficult experiments

1 SNU (solar neutrino unit) 10^{-36} neutrino captures per target atom per second

1 ton target with mass number A=20
number of atoms $10^6\ N_A/A \sim 3\times10^{28}$
less than 1 neutrino interaction per year for 1 SNU

Solar Neutrinos: A Scientific Puzzle

John N. Bahcall and Raymond Davis, Jr.

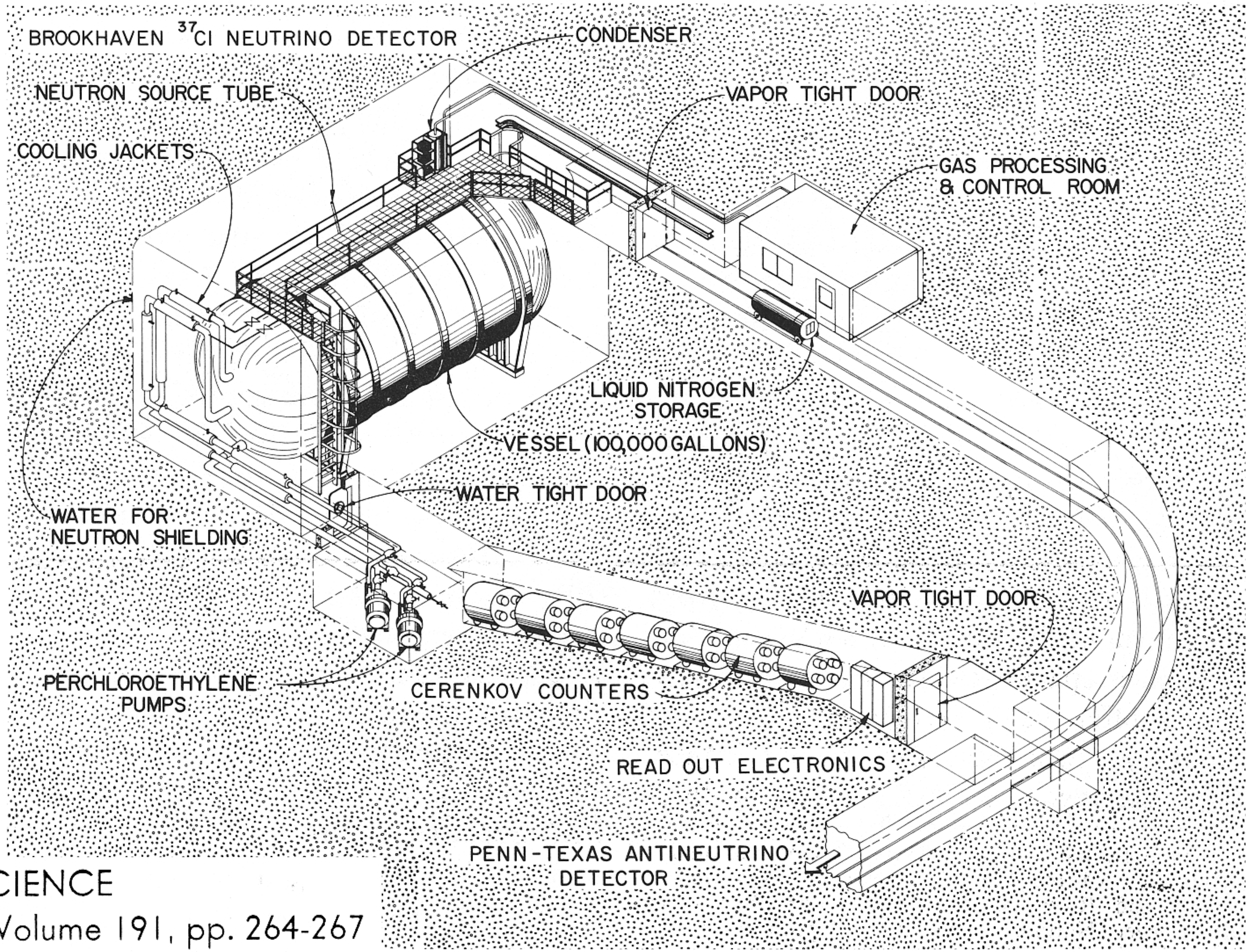

Reprinted from SCIENCE
23 January 1976, Volume 191, pp. 264-267

Ray Davis shows John Bahcall the tank containing 100,000 gallons of perchloroethylene. The picture was taken in the Homestake mine shortly before the experiment began operating.

615 tons of C_2Cl_4 operated for 30 years

$$\nu_e + {}^{37}\mathrm{Cl} \longrightarrow {}^{37}\mathrm{Ar} + e^-$$

threshold 0.814 MeV

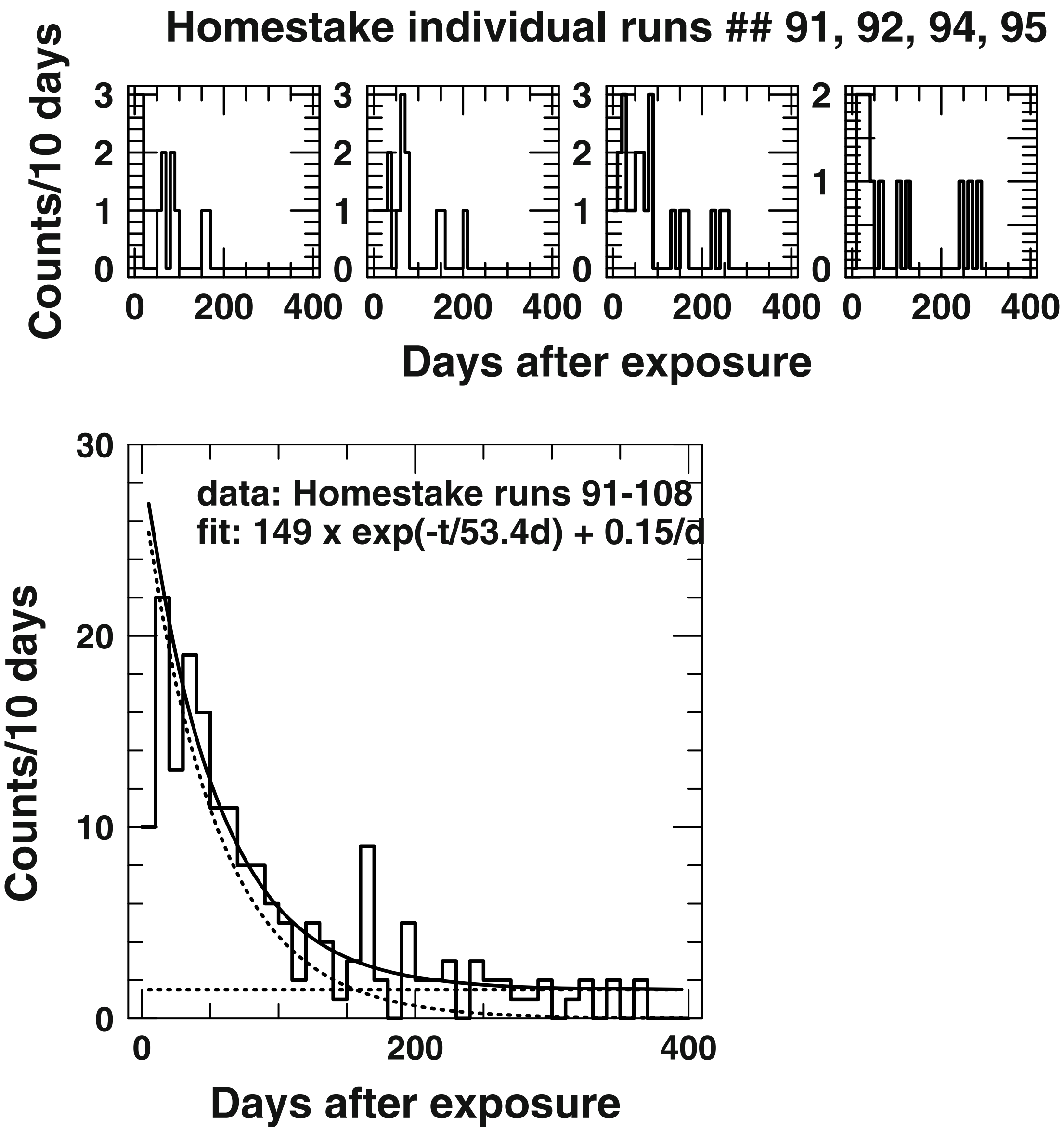

Fig. 3.2. The upper panel shows the results from four individual counting periods of the Homestake tank: ## 91, 92, 94 and 95. The lower panel shows the time dependence of the counting rate for 14 runs.

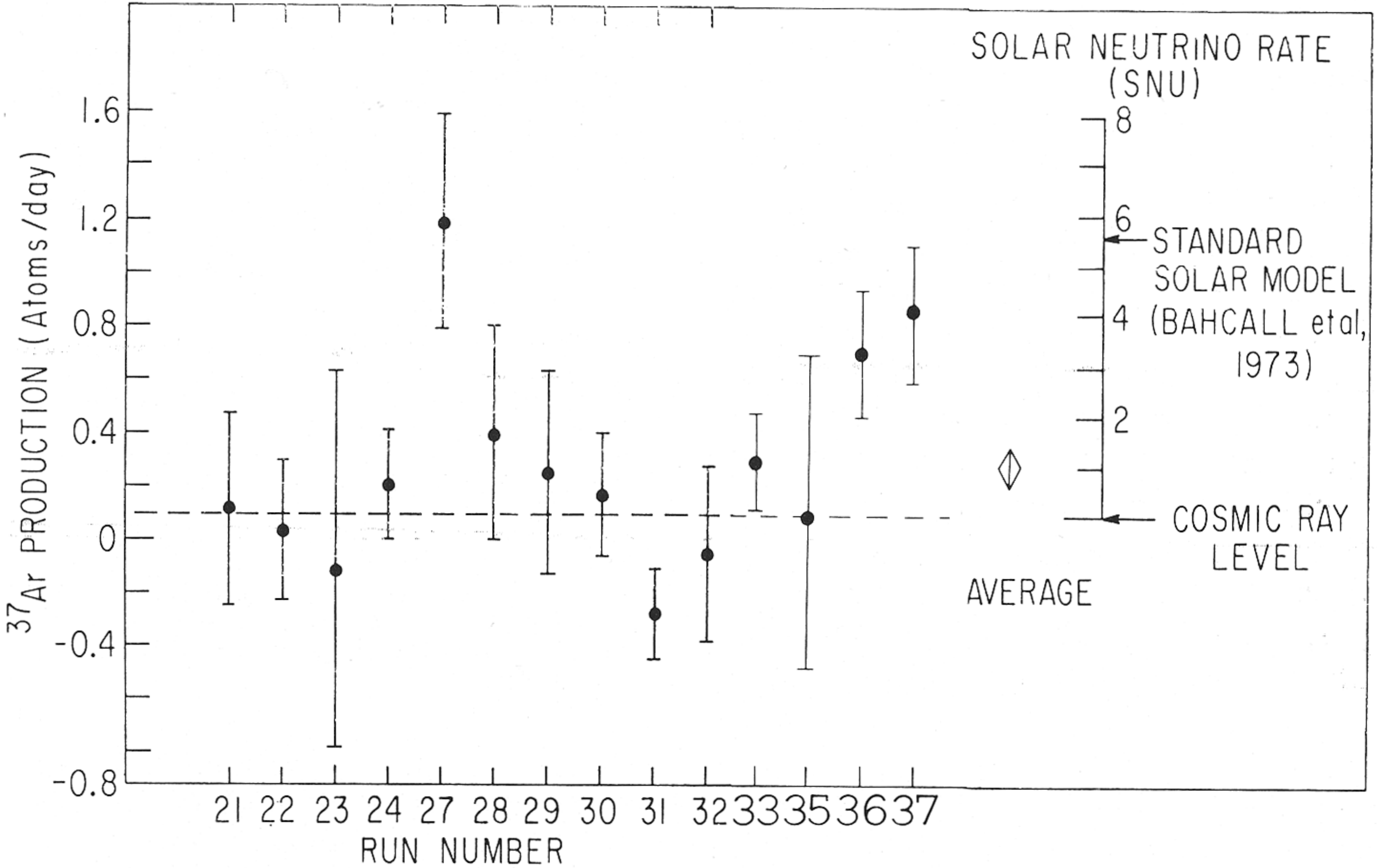

Fig. 2. Summary of the neutrino observations.

Reprinted from SCIENCE
23 January 1976, Volume 191, pp. 264-267

Solar neutrino detection

GALEX and SAGE

$$\nu_e + {}^{71}\mathrm{Ga} \longrightarrow {}^{71}\mathrm{Ge} + e^-$$

threshold 0.232 MeV —> detection of pp neutrinos

GALEX: 30 tons gallium
SAGE: 57 tons gallium

—> measured ~70 SNU (SSM predicts ~130 SNU)
—> experimental prove that pp chain is main source of solar energy

Neutrino scattering

neutrino scattering reaction $\nu_e + e^- \longrightarrow \nu_e + e^-$

scattered electron carries large fraction of neutrino energy and moves in direction close to initial direction of neutrino

cross section $9.3 \times 10^{-45}\ \mathrm{cm}^2 \times (\mathrm{E}_\nu/\mathrm{MeV})^2.$

Kamiokande experiment, Super-Kamiokande
threshold, originally 7.5 MeV, gradually lowered to 6.5 MeV

—> ~13 neutrinos/day from Sun

~30 t typical size of a neutrino detector

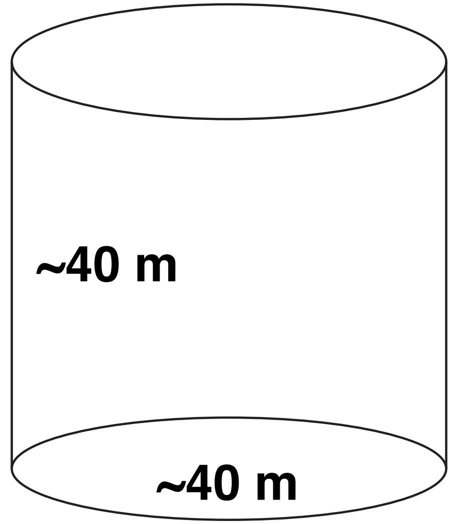

e.g. Super Kamiokande (50 000 t)
ultra-pure water (~30000 PMTs)

method: neutrino-electron scattering

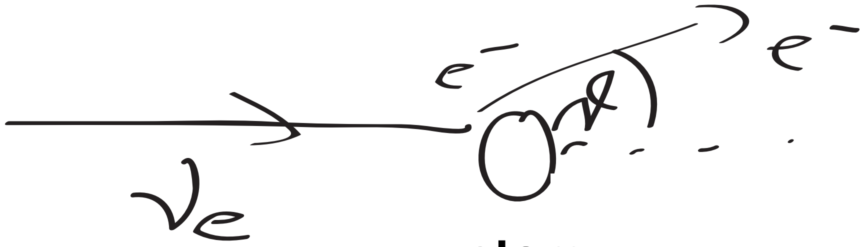

$$\sigma_{\nu e} \approx 10^{-43}\ \mathrm{cm}^2 \left(\frac{E_\nu}{10\ \mathrm{MeV}} \right)$$

electrons are boosted in forward direction

$$\cos\vartheta = \frac{1 + \frac{m_e}{E_\nu}}{\sqrt{1 + \frac{2m_e}{E'_e}}}$$

E_e' **kinetic energy of recoil electron (Compton)**

measurement of the electron via Cherenkov radiation in water

$$\cos\Theta_c = \frac{1}{\beta n} \quad \mathrm{H_2O} : n = 1.33 \Rightarrow \Theta_c = 42^\circ$$

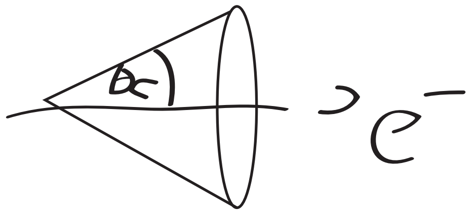

threshold $E_\nu > 7.5\ \mathrm{MeV}$

Super Kamiokande

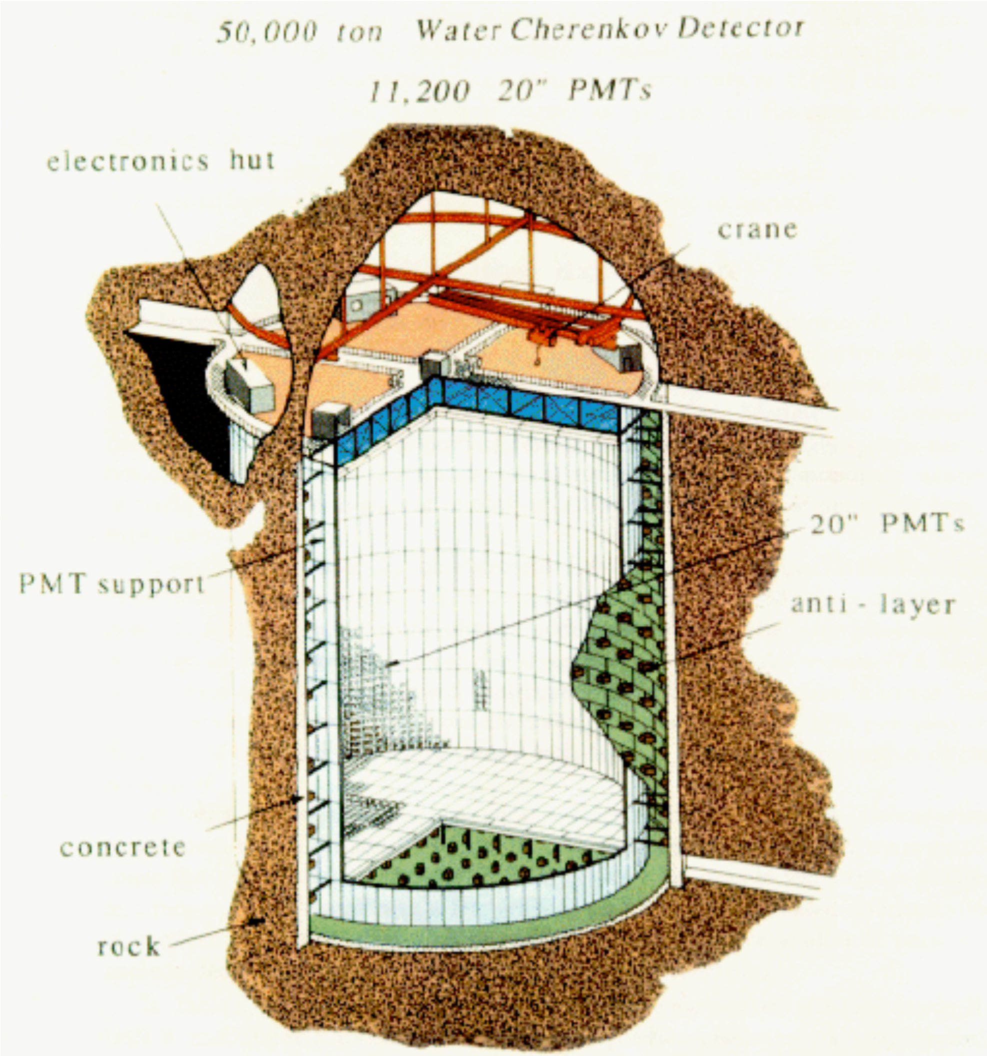

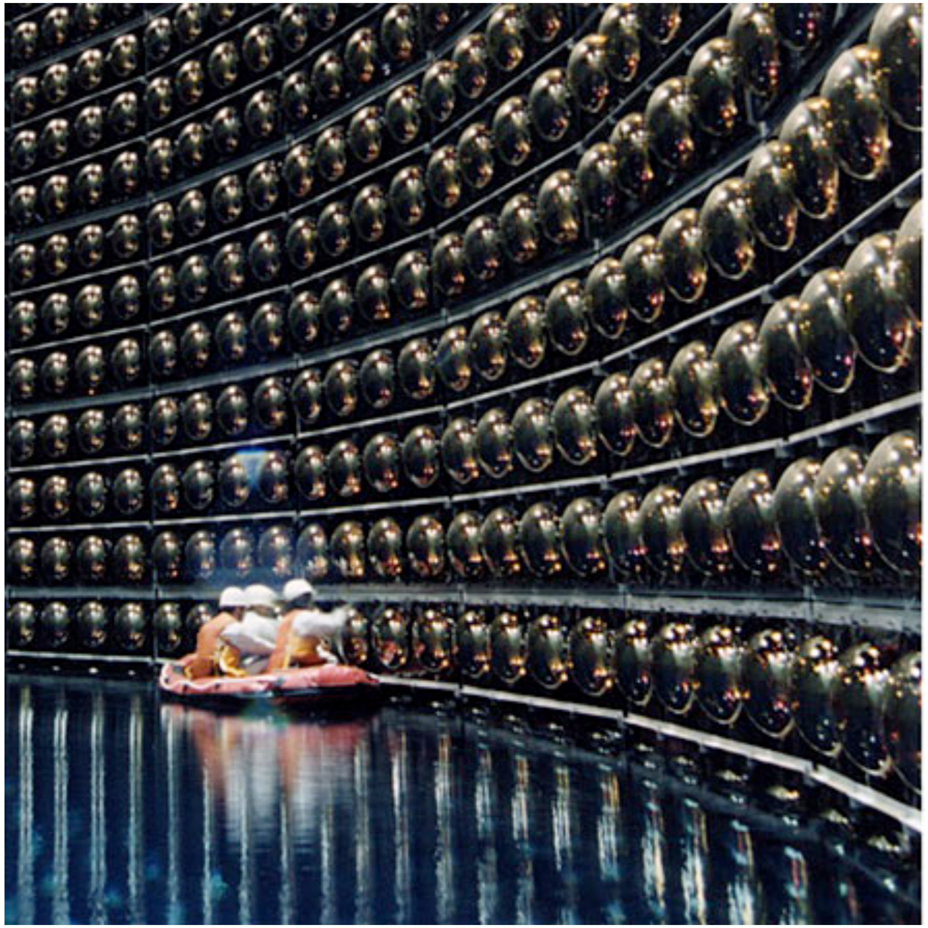

Super Kamiokande

electron **muon**

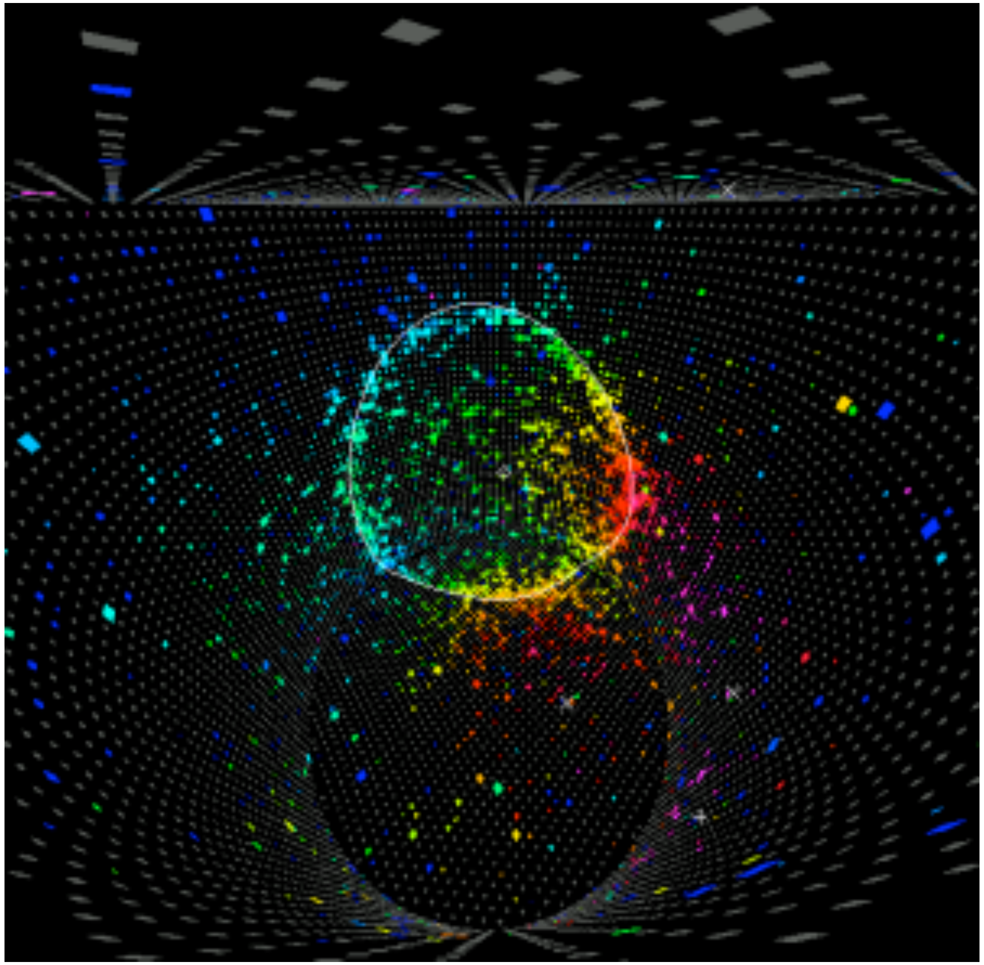

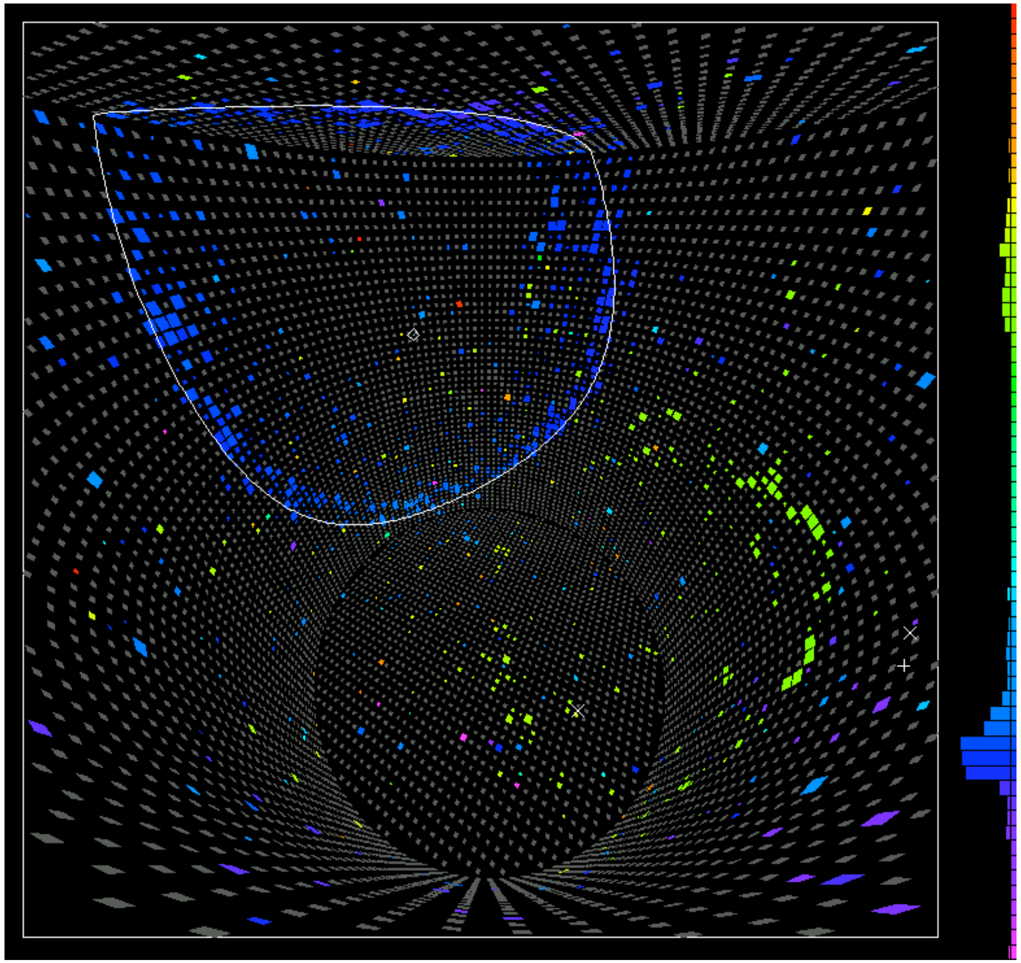

Super Kamiokande

sun in neutrino „light“

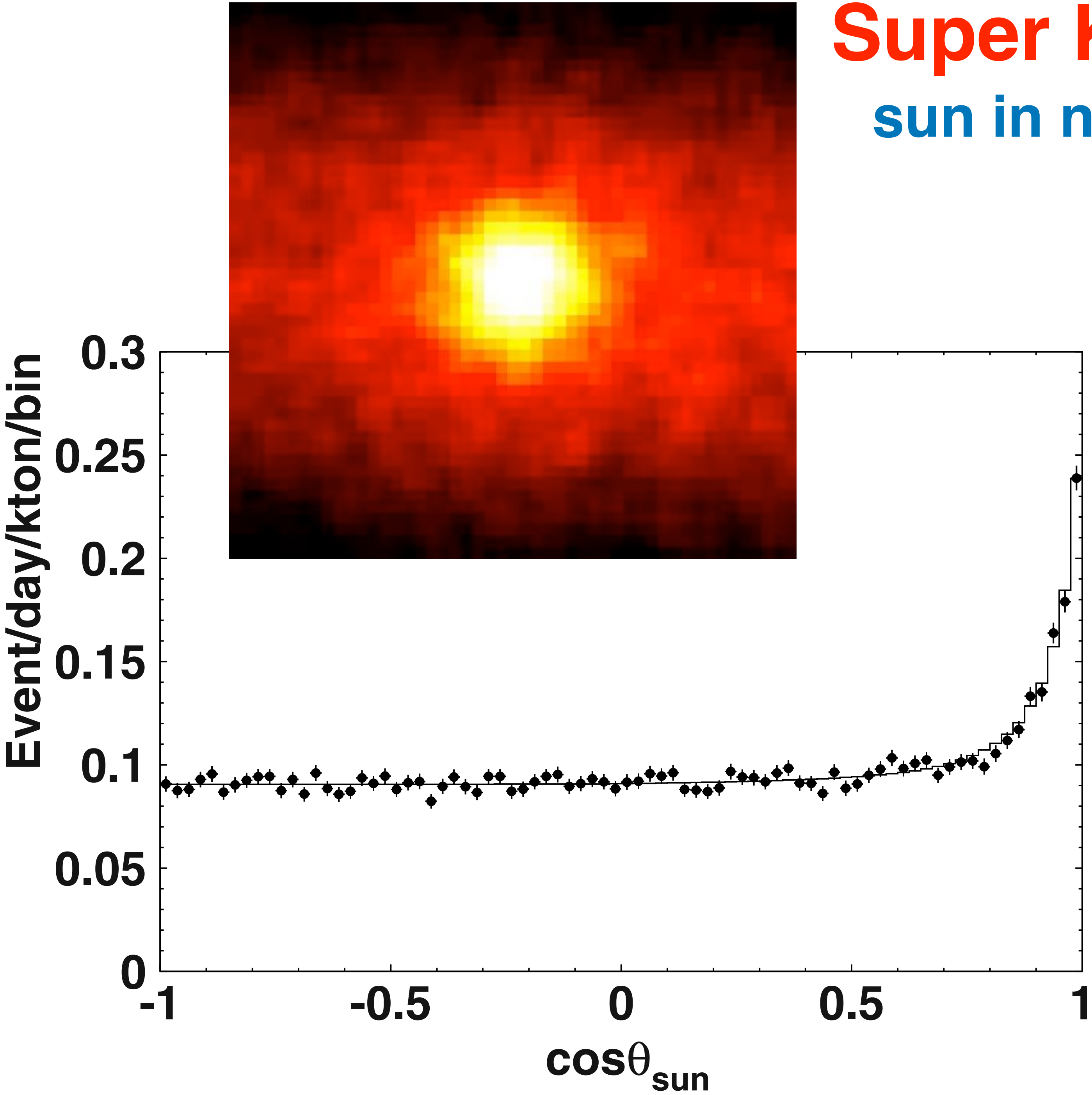

Fig. 3.1. Angular distribution of Super-Kamiokande neutrino events with respect to the direction of the Sun at the time of detection.

experiments measure less solar neutrinos than expected —> solar neutrino puzzle

solution: neutrino oscillations —> *will discuss later*

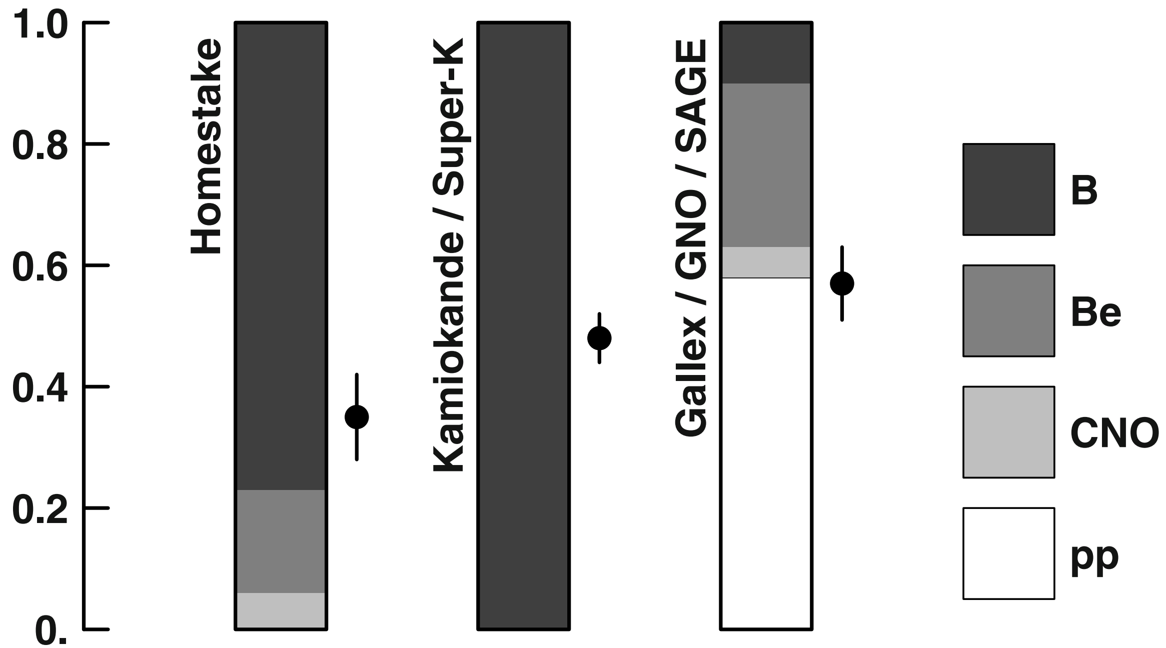

Fig. 3.3. Predictions of the contribution of different reactions to the neutrino rates in different types of detectors are compared to the observed rates.

Stellar evolution

stellar luminosity proportional to mass $L \propto M^n \quad n \simeq 3$

Hertzsprung-Russel diagram
luminosity vs surface temperature

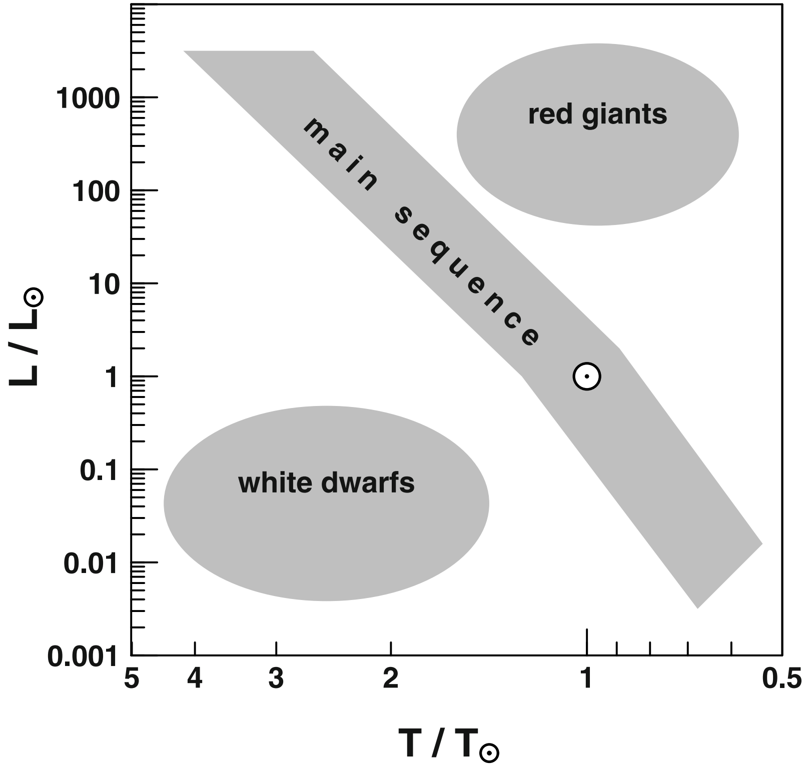

Fig. 3.4. This is a cartoon of a HR diagram, which usually consists of a scatter plot of measured stellar parameters. Note the position of the Sun at unit surface temperature and luminosity. Note also that in a classical astronomical fashion the temperature increases from right to left.

stars stay on main sequence until ~10% of their mass is exhausted in the fusion of helium

massive stars spend less time on main sequence, duration ~M^{-3}

sun ~10 billion years
$20M_\odot$ **only ~1 million years**

Supernova explosions

massive stars ($M > 1.4\ M_{sun}$)
e.g. 20 M_{sun}: subsequent fusion of heavy elements up to iron
—> upper right corner of HRD

high density and temperature in center of star
—> new radiation process: neutrino emission
photons generate electron-positron pairs through collisions with matter
—> neutrinos can leave star unscattered (low cross section)
—> energy lost for hydrostatic equilibrium

some of the heavy elements disintegrate —> consumes energy/decreasing pressure

electrons and protons interact —> neutrons $e^- + p \;=\; n + \nu_e.$

core (~ inner 1.4 solar masses) of star collapses

collapsing region decreases to about 50 km
—> central density exceeds nuclear density $10^{14}\ \mathrm{g/cm^3}.$

inner core bounces back, shock propagates outwards, carries 10^{51} ergs of energy
—> Supernova explosion

Core-Collapse Supernova Explosion

Massive stars collapse ejecting the outer mantle by means of shock-wave driven explosions.

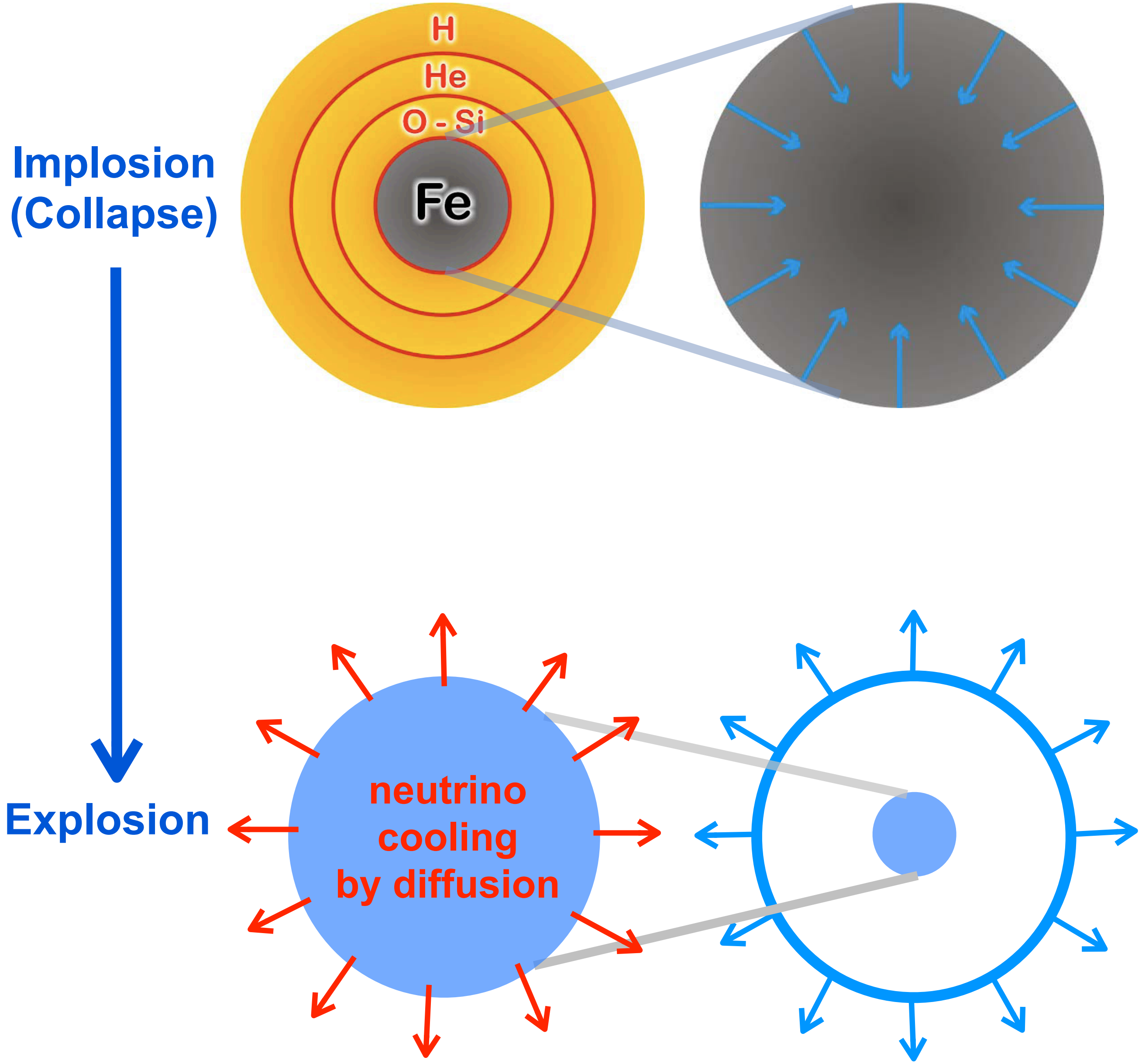

Neutrinos carry 99% of the released energy (~ 10^{53} erg).

radiate away binding energy

Neutrino energies: ~ 10 MeV.
Neutrino emission time: ~ 10 s.

Supernova neutrinos

binding energy radiated away through neutrinos

high densities in core
pair production of particles and scattering
electron neutrinos and anti neutrinos scatter on average ~10000 times

as neutrinos cool down to 20-30 MeV they can escape from the porto-neutron star

$$E_{\nu_e} \ : \ E_{\bar{\nu}_e} \ : \ E_{\nu_\mu} \ = \ 1.2 \ : \ 1 \ : \ 4 \ ,$$

SN1987A in large Magellanic cloud (23 February 1987) **d ~50 kpc**

for binding energy of $E_{bind} = 2\text{–}4 \ \times 10^{53} \ \mathrm{ergs}$

and monoenergetic neutrinos (15 MeV) the flux at Earth should contain

$$F_\nu \ = \ \frac{E_b}{15\mathrm{MeV}} \frac{1}{4\pi(50\mathrm{kpc})^2} \simeq 3 - 6 \times 10^{10}\ \mathrm{cm}^{-2}$$

neutrinos of all flavors during about 10 sec

Neutrinos from SN 1987a

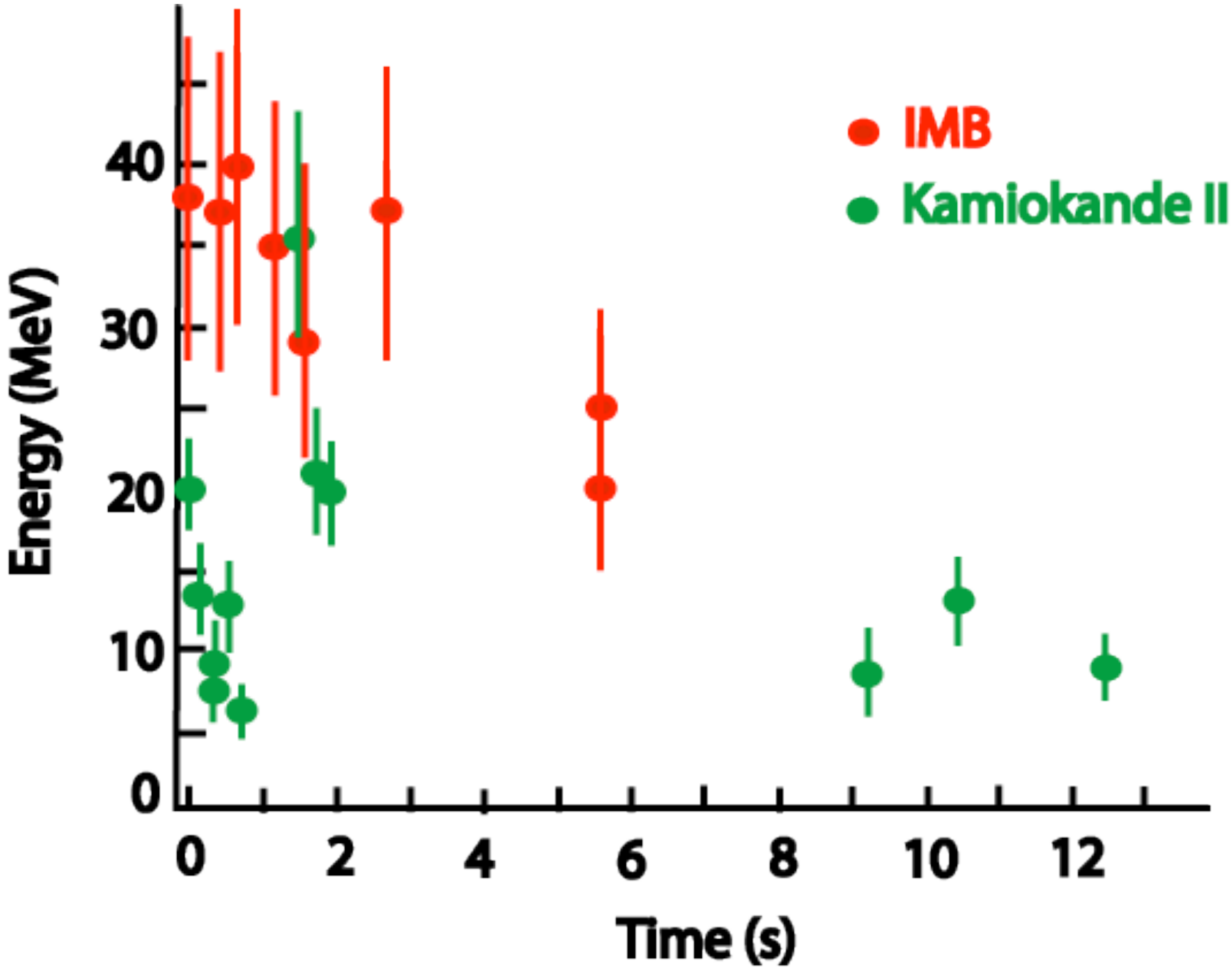

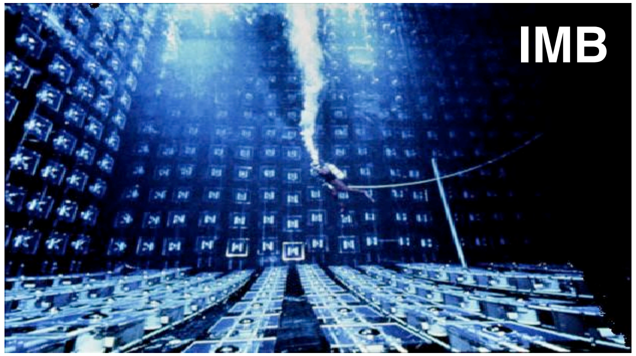

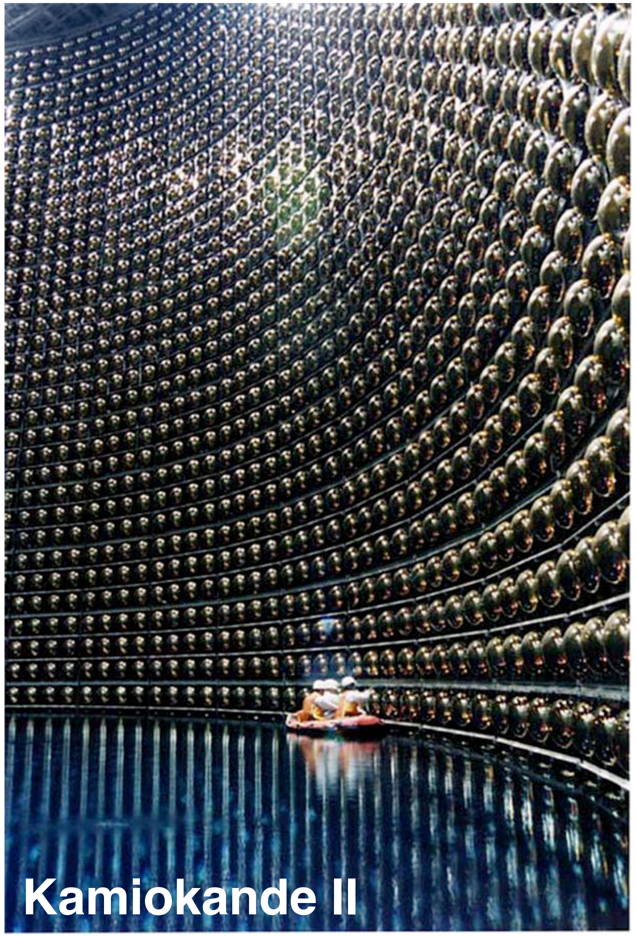

Neutrinos from SN 1987a

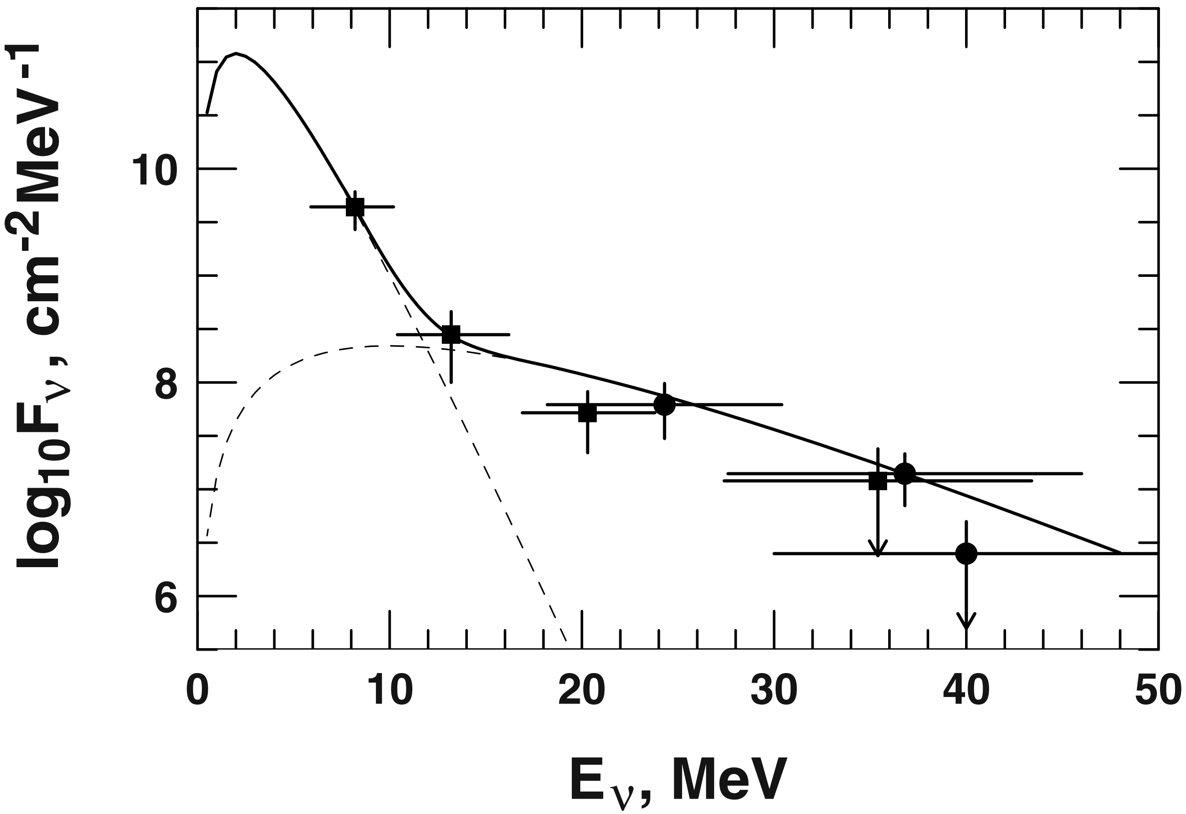

Fig. 3.6. Energy spectrum of the supernova neutrinos. The Kamiokande data are plotted with squares and IMB – with dots. The two dashed lines represent black body spectra with temperatures 1.5 and 5 MeV and the solid line is their sum.

detailed calculations and models: T = 4.1 MeV $E_\nu = 4.5 \times 10^{52}$ *ergs.*

accounting for energy of non-interacting neutrinos, total neutrino energy from SN1987A is 3×10^{53} *ergs,*

Are We Ready For the Next SN Explosion?

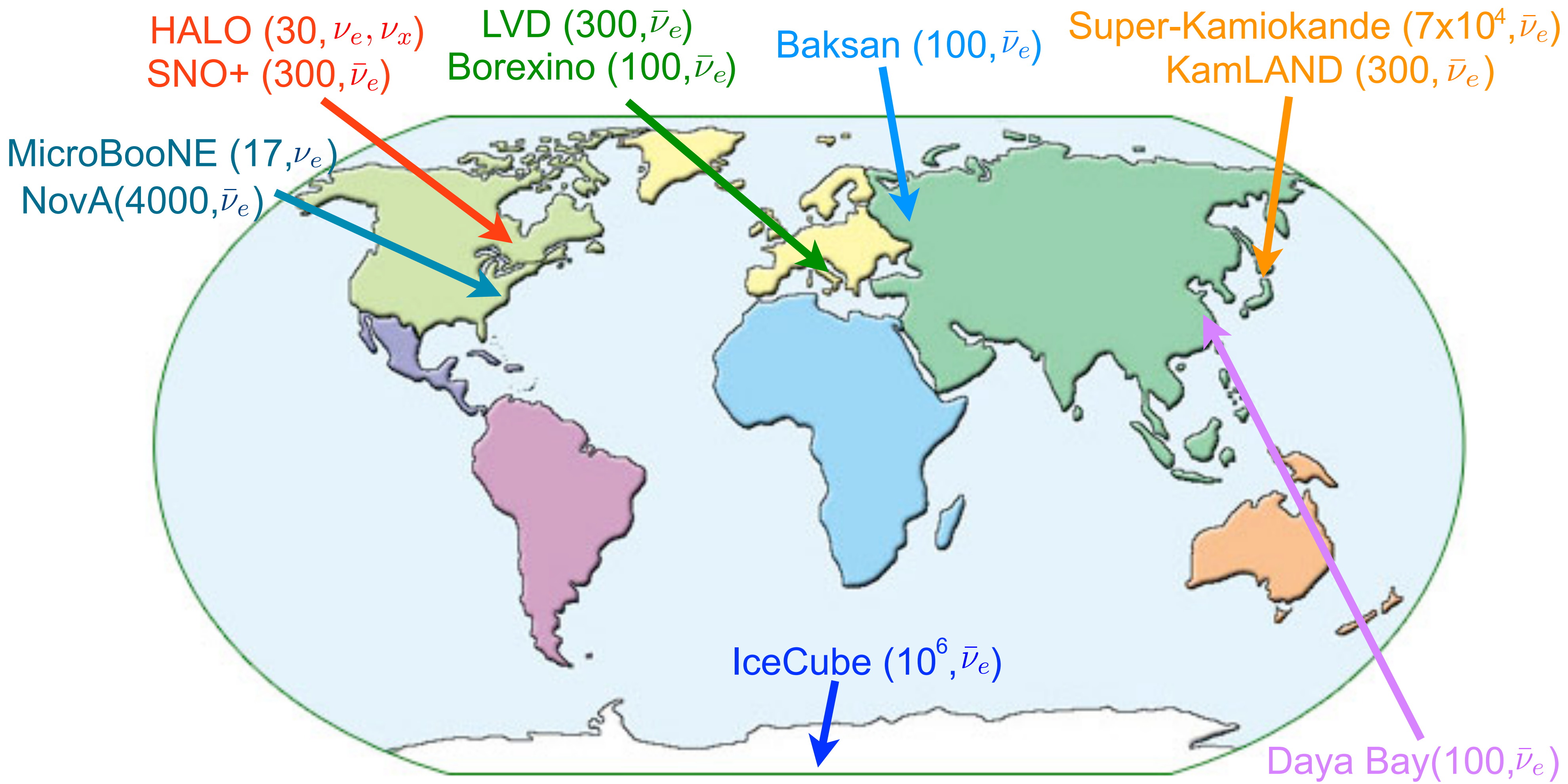

Expected number of events for a SN at 10 kpc and dominant flavor sensitivity in parenthesis.

Fundamental to combine the SN signal seen in detectors employing different technologies.

Recent review papers: Scholberg (2012). Mirizzi, Tamborra, Janka, Scholberg et al. (2016).

Supernova remnants

SN1006

Crab nebula 1054

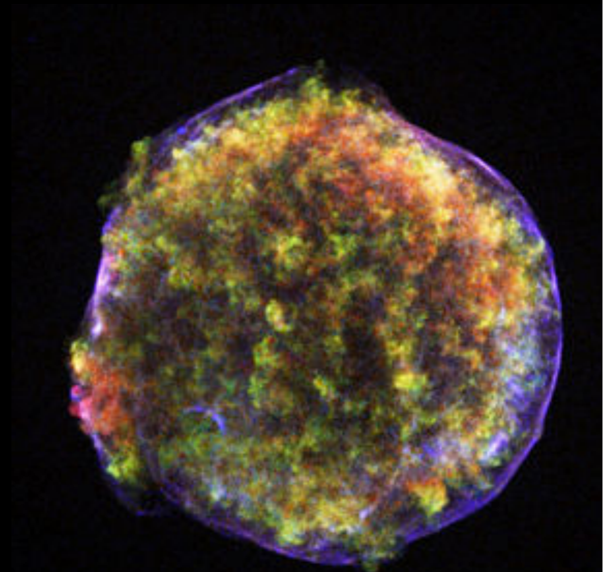

Tycho’s supernova 1572

6 supernovae observed in last millenium in Galaxy and LMC

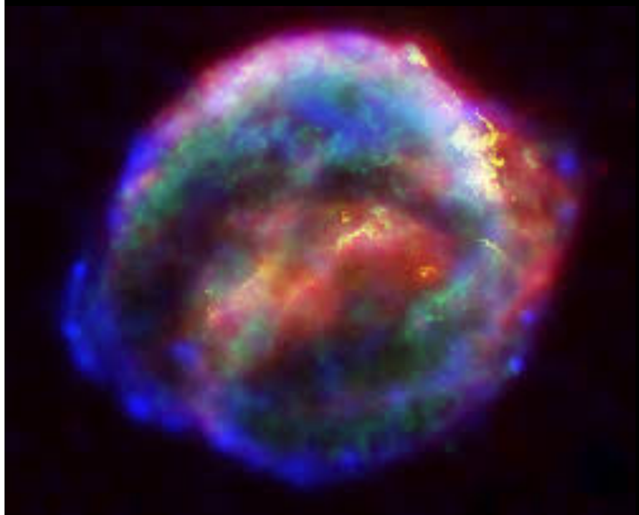

Kepler’s supernova 1604

Cas A 1680

Cassiopeia A

X-ray

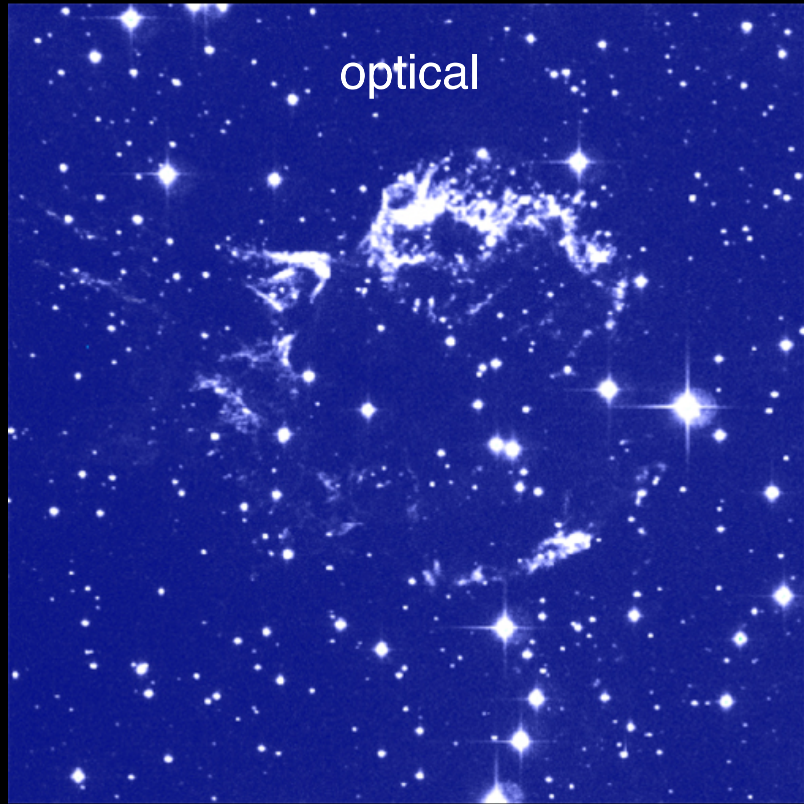

infrared

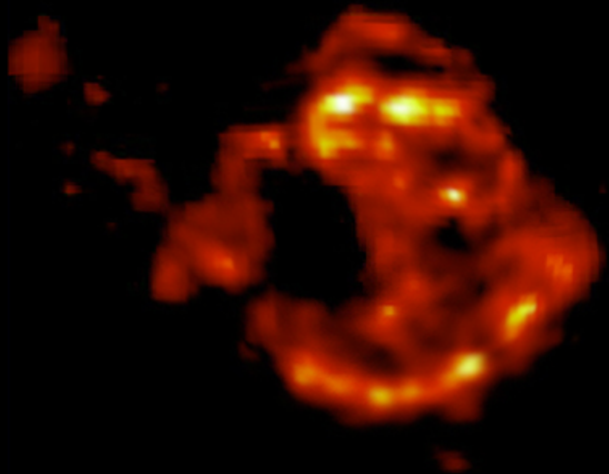

radio

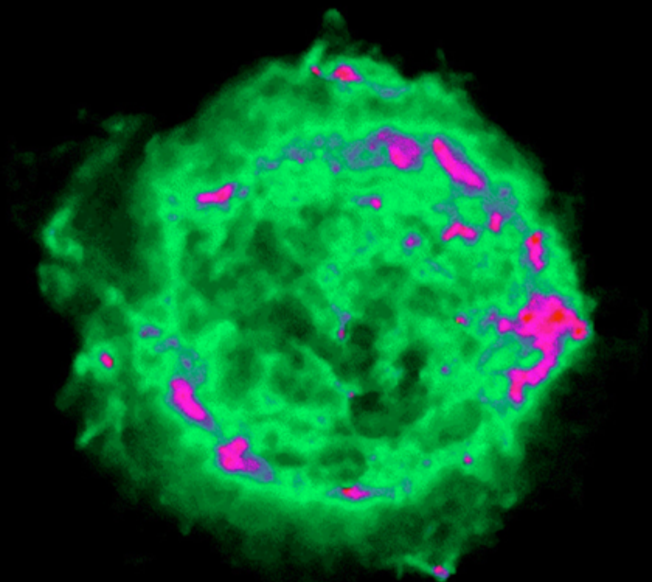

optical light curve of SN1987A during first 3 years

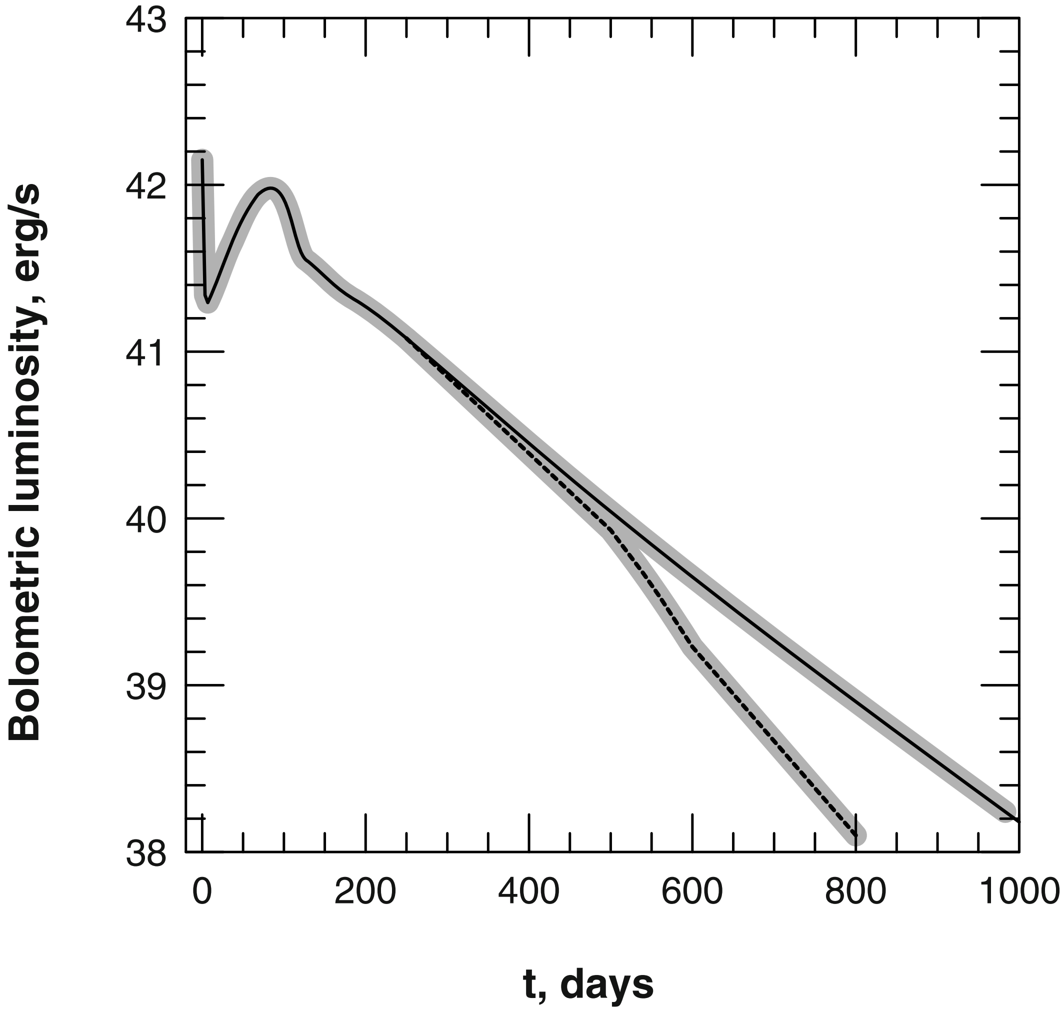

Fig. 3.7. The bolometric luminosity of SN1987a during the first 1,000 days after the explosion. The lower branch after $\sim$ 400 days shows the optical luminosity and the upper branch adds the optical, X-ray and the γ-ray luminosities.

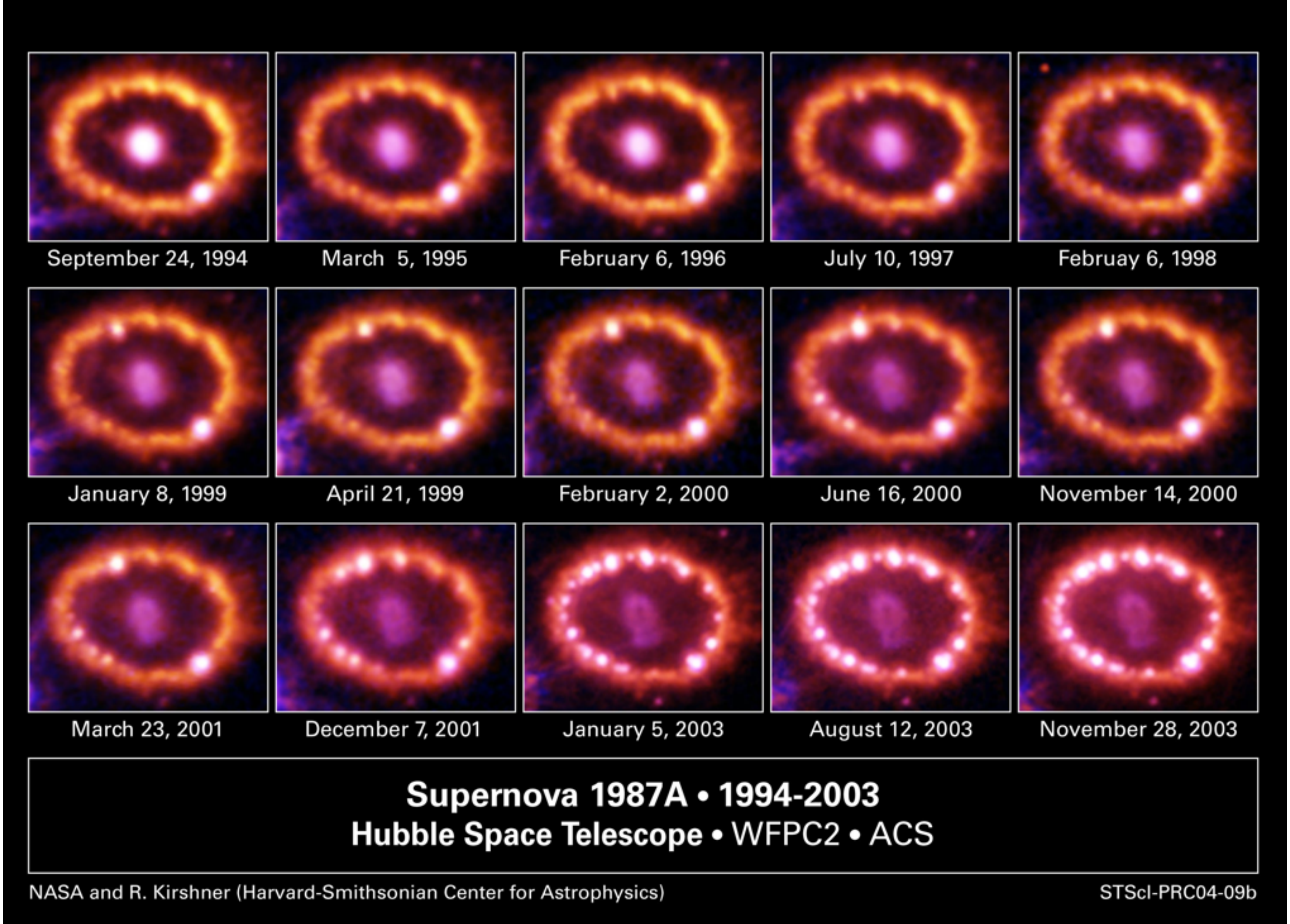
September 24, 1994
March 5, 1995
February 6, 1996
July 10, 1997
Februay 6, 1998
January 8, 1999
April 21, 1999
February 2, 2000
June 16, 2000
November 14, 2000
March 23, 2001
December 7, 2001
January 5, 2003
August 12, 2003
November 28, 2003
Supernova 1987A • 1994-2003
Hubble Space Telescope • WFPC2 • ACS
NASA and R. Kirshner (Harvard-Smithsonian Center for Astrophysics)
STScI-PRC04-09b

Acceleration of cosmic rays

kinetic energy of SNR is converted to cosmic rays

volume of Galactic disc $\pi\,(15\text{ kpc})^2(500\text{ pc}) \quad \sim\ 10^{67}\ \text{cm}^3$

energy density of cosmic rays $0.5\ \text{eV}/\text{cm}^3. \qquad t_{GD} = 10^7\ \text{years}$

we will discuss later measurements of this quantity

power of cosmic rays:

$$L_{CR} = \frac{v_{GD} \times \rho_E}{t_{GD}} \simeq 3 \times 10^{40}\ \text{erg/s}.$$

Three supernova remnants of mass $10 M_\odot$ expanding with velocity of 5×10^8 cm/s per century would produce 3×10^{42} erg/s. Thus an acceleration efficiency of only 1% would supply the energy content of the cosmic rays in the galactic disk.

—> SNR are attractive candidates for cosmic-ray acceleration

On the Origin of the Cosmic Radiation

ENRICO FERMI
Institute for Nuclear Studies, University of Chicago, Chicago, Illinois
(Received January 3, 1949)

A theory of the origin of cosmic radiation is proposed according to which cosmic rays are originated and accelerated primarily in the interstellar space of the galaxy by collisions against moving magmetic fields. One of the features of the theory is that it yields naturally an inverse power law for the spectral distribution of the cosmic rays. The chief difficulty is that it fails to explain in a straightforward way the heavy nuclei observed in the primary radiation.

I. INTRODUCTION

IN recent discussions on the origin of the cosmic radiation E. Teller[1] has advocated the view that cosmic rays are of solar origin and are kept relatively near the sun by the action of magnetic fields. These views are amplified by Alfvén, Richtmyer, and Teller.[2] The argument against the conventional view that cosmic radiation may extend at least to all the galactic space is the very large amount of energy that should be present in form of cosmic radiation if it were to extend to such a huge space. Indeed, if this were the case, the mechanism of acceleration of the cosmic radiation should be extremely efficient.

I propose in the present note to discuss a hypothesis on the origin of cosmic rays which attempts to meet in part this objection, and according to which cosmic rays originate and are accelerated primarily in the interstellar space, although they

where H is the intensity of the magnetic field and ρ is the density of the interstellar matter.

One finds according to the present theory that a particle that is projected into the interstellar medium with energy above a certain injection threshold gains energy by collisions against the moving irregularities of the interstellar magnetic field. The rate of gain is very slow but appears capable of building up the energy to the maximum values observed. Indeed one finds quite naturally an inverse power law for the energy spectrum of the protons. The experimentally observed exponent of this law appears to be well within the range of the possibilities.

The present theory is incomplete because no satisfactory injection mechanism is proposed except for protons which apparently can be regenerated at least in part in the collision processes of the cosmic radiation itself with the diffuse interstellar matter.

Stochastic acceleration of charged particles

relativistic particle scattered at magnetic could

The particle energy in the coordinate system of the cloud is

$$E_0^* = \gamma_{cl}(E_0 + \beta_{cl} p_0) \, ,$$

The energy of the particle E_1 at the time it exits the cloud will be

$$E_1 = \gamma_{cl}(E_0^* + \beta_{cl} p_0^*) = E_0 \times \gamma_{cl}^2 (1 + \beta_{cl})^2$$

The particle has gained energy ΔE. The relative gain

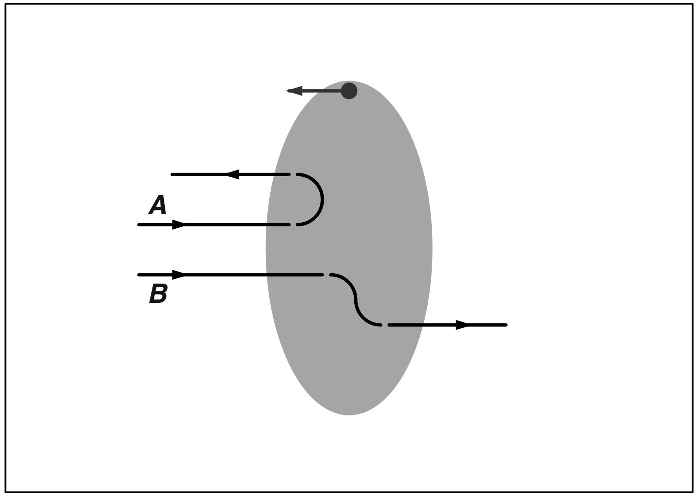

$$\frac{\Delta E}{E} = \frac{E_1 - E_0}{E_0} = \gamma_{cl}^2 (1 + \beta_{cl})^2 - 1 \equiv \xi$$

energy gain proportional to speed of cloud squared
—> second order Fermi acceleration

for all scattering angles

energy gain per cloud encounter then becomes $\xi \simeq 4/3 \, \beta_{cl}^2$.

Fig. 3.8. Schematic representation of Fermi's idea of particle acceleration by scattering in magnetized clouds. Only the case when the particle trajectories are collinear with the cloud velocity are shown.

Stochastic acceleration of charged particles

It is important to remember that the fractional energy gain in the process of stochastic acceleration is constant. After n encounters of magnetic clouds (with the same β_{cl} for simplicity) the particle energy will be

$$E_n = E_0(1+\xi)^n$$

and the number of encounters needed to reach energy E_n is respectively

$$n = \ln\left(\frac{E_n}{E_0}\right) / \ln(1+\xi).$$

at every encounter particle can escape $(1 - P_{esc})^n$

$$N(>E_n) = N_0 \sum_n^{\infty} (1 - P_{esc})^m \propto A \left(\frac{E_n}{E_0}\right)^{-\gamma}$$

power law

with

$$\gamma \simeq P_{esc}/\xi.$$

The energy gain per unit time depends on the frequency of encounters ν_{enc} and is

$$\frac{dE}{dt} = \nu_{enc}\Delta E = \frac{c}{\lambda_{enc}}\xi E = \frac{\xi E}{T_{enc}} \tag{3.18}$$

where λ_{enc} is the mean free path between encountering magnetic clouds and T_{enc} is the characteristic time per encounter.

problems:

1) typical velocity of interstellar clouds

$$\frac{V}{c} \approx 10^{-4} \rightarrow \left\langle \frac{\Delta E}{E} \right\rangle \approx 2.6 \cdot 10^{-8}$$

2) mean free path of CRs

$$\lambda = \frac{3D}{v} = \frac{3 \cdot 10^{28} \ \frac{\mathrm{cm}^2}{\mathrm{s}}}{3 \cdot 10^{10} \ \frac{\mathrm{cm}}{\mathrm{s}}} = 10^{18} \ \mathrm{cm} = 0.3 \ \mathrm{pc}$$

example:
accelerate particles from 1 GeV to 1 PeV

$$\frac{E'}{E} = 10^6 \rightarrow \left(1 + \frac{\Delta E}{E}\right)^k = 10^6$$

$$\approx 2.6 \cdot 10^{-8}$$

$$\rightarrow k \approx 0.5 \cdot 10^9 \qquad \rightarrow t \approx 0.5 \cdot 10^9 \ \mathrm{a}$$

process too slow
‘age‘ of CRs ~10^7 a

energy losses through ionization etc. are stronger than energy gain

1st order Fermi acceleration

1977: Effective acceleration in connection with strong shocks if plasma moves with supersonic velocity through ISM.
Such conditions can be found in supernova explosions.

Shock waves are a general phenomenon if particles or plasma clouds move at supersonic velocities

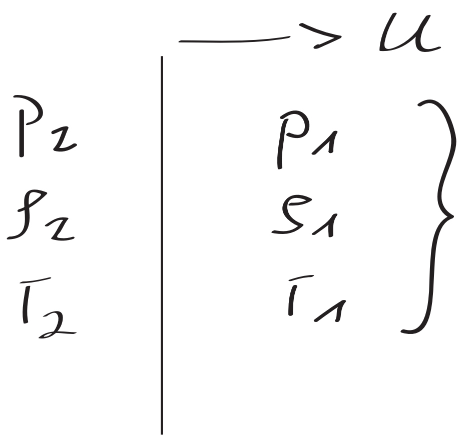

***U* supersonic**

resting gas

shock front

examples of ideal shocks:

- **interplanetary shock against the solar wind or**
- **bow shock of solar system**

supersonic shock

structure of Earth's magnetosphere

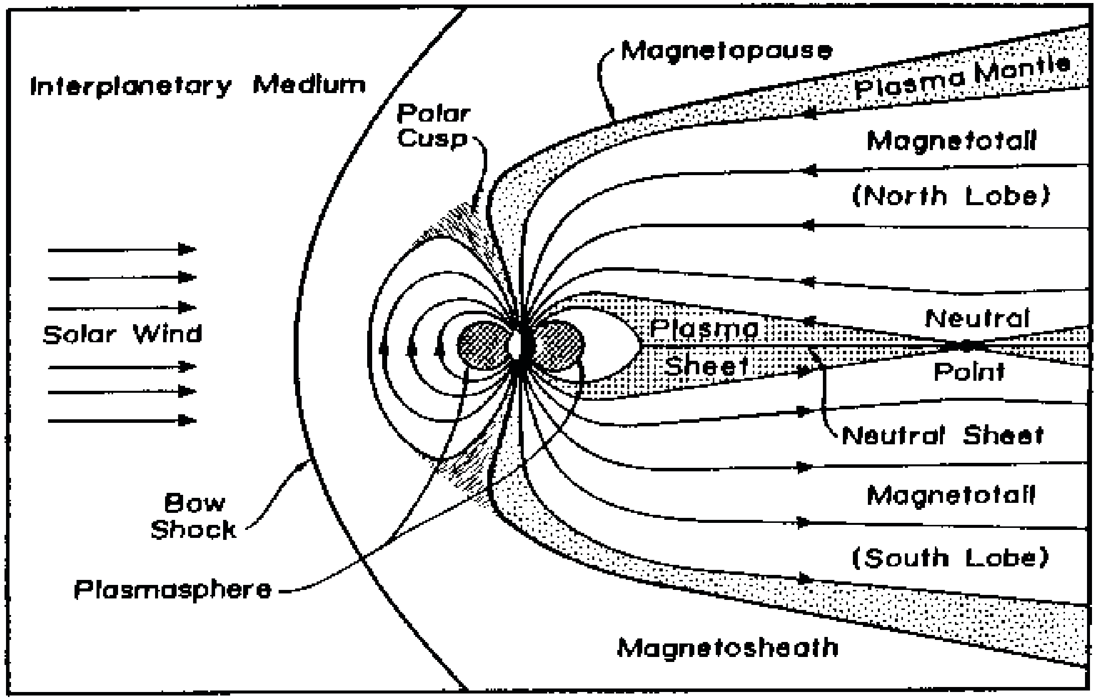

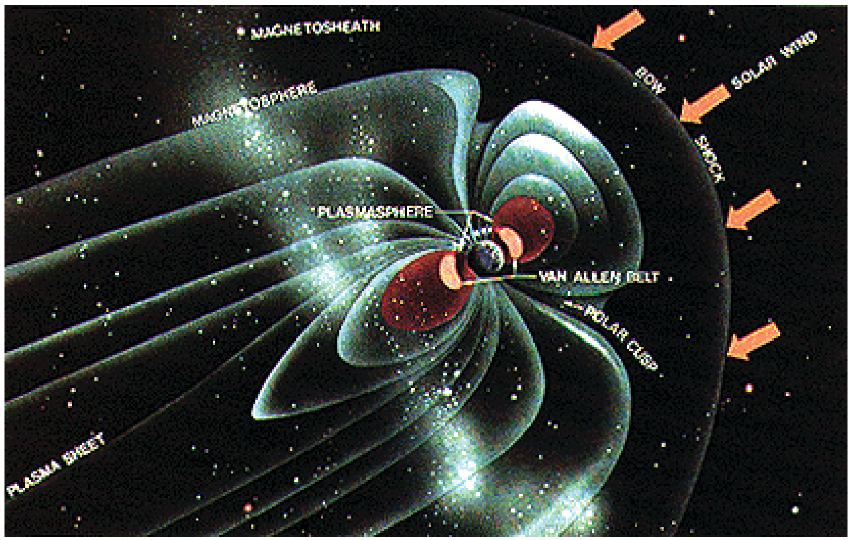

SOHO observation of an interplanetary shock

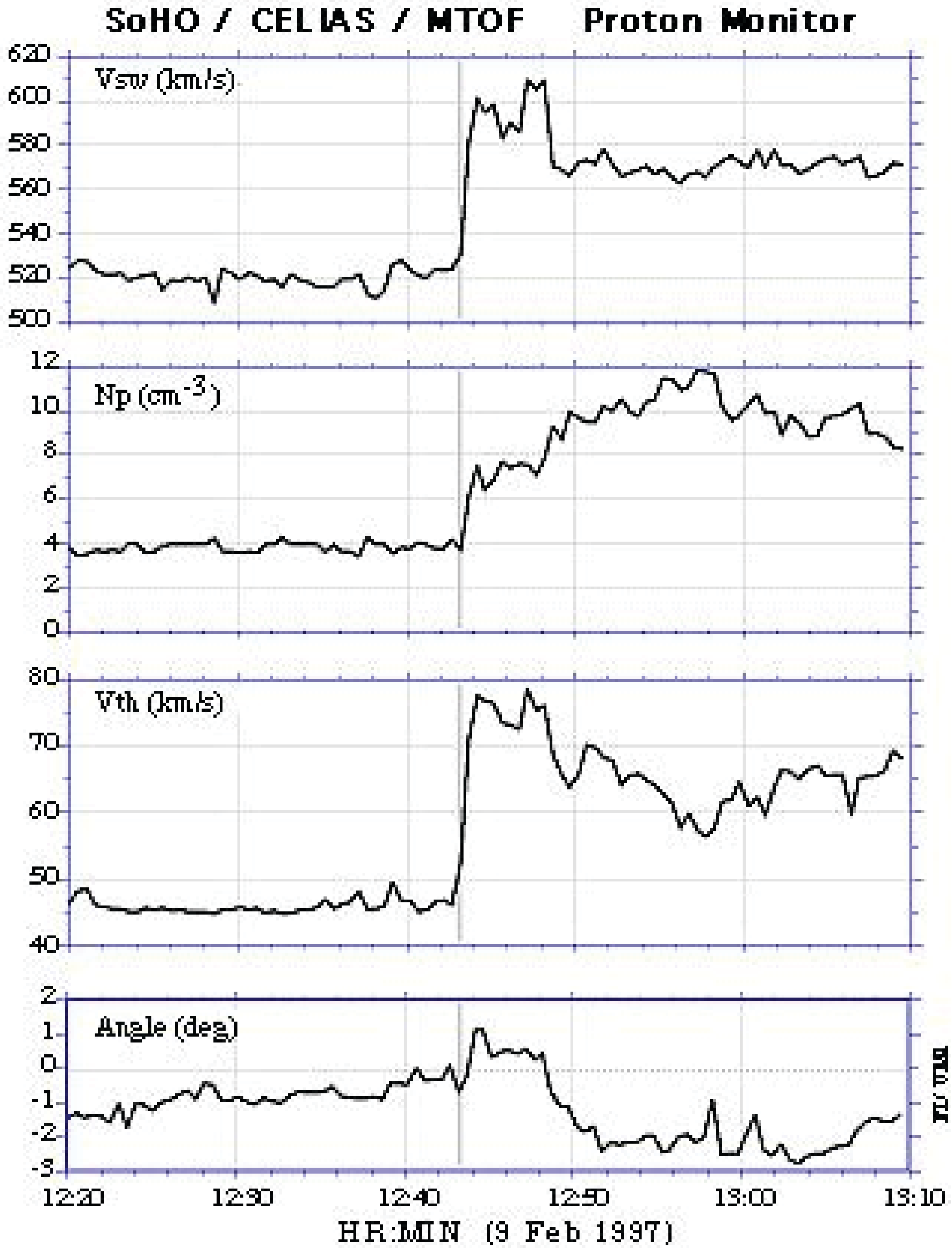

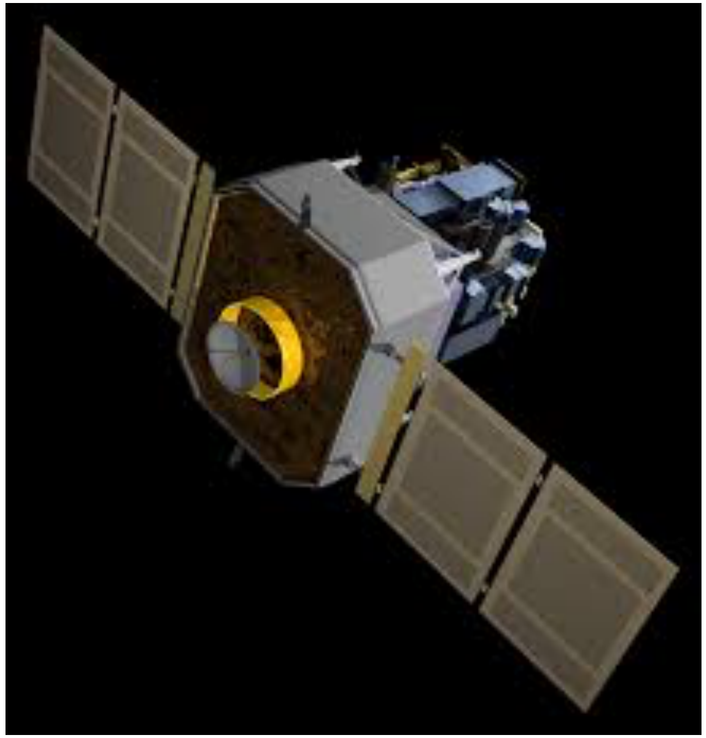

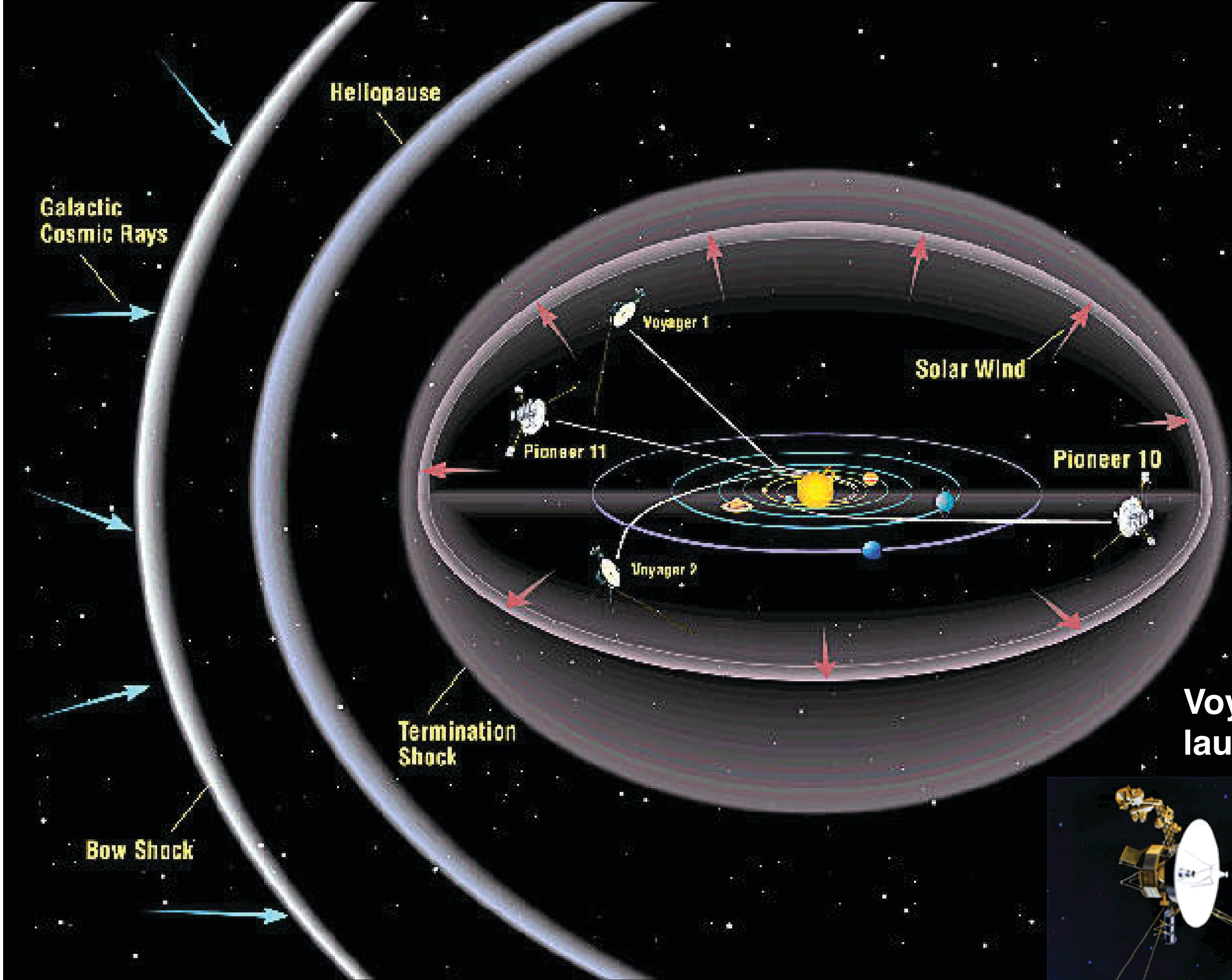

Voyager 1+2 launched 1977

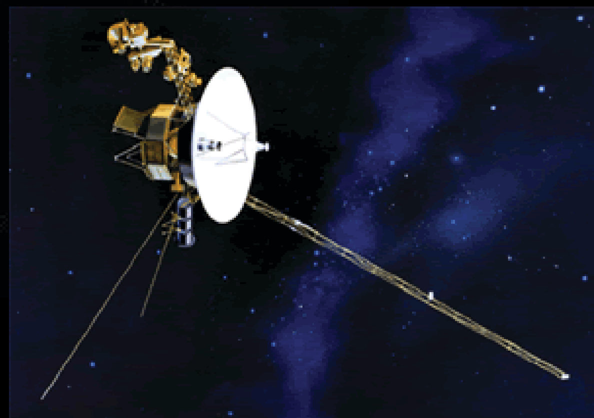

Particle acceleration at astrophysical shocks

shock ahead of expanding SNR is formed because expansion velocity of the remnant v_R is much higher than the sound velocity of the ISM

ISM at shock is ionized
—> shock velocity $$v_S \simeq 4/3 v_R$$

strength of shock is characterized by compression ratio

$$R \simeq \frac{v_S/v_R}{v_S/v_R - 1} \text{ and } R = 4 \text{ in this case.}$$

If the radial dimensions of the shock are much larger than the particle gyroradius r_g

$$r_g = pc/ZeB \simeq 3.2 \times 10^6 \mathrm{cm} \times (E/\mathrm{GeV})/(B/\mathrm{G}) ,$$

—> shock is represented as plane for the purpose of particle acceleration

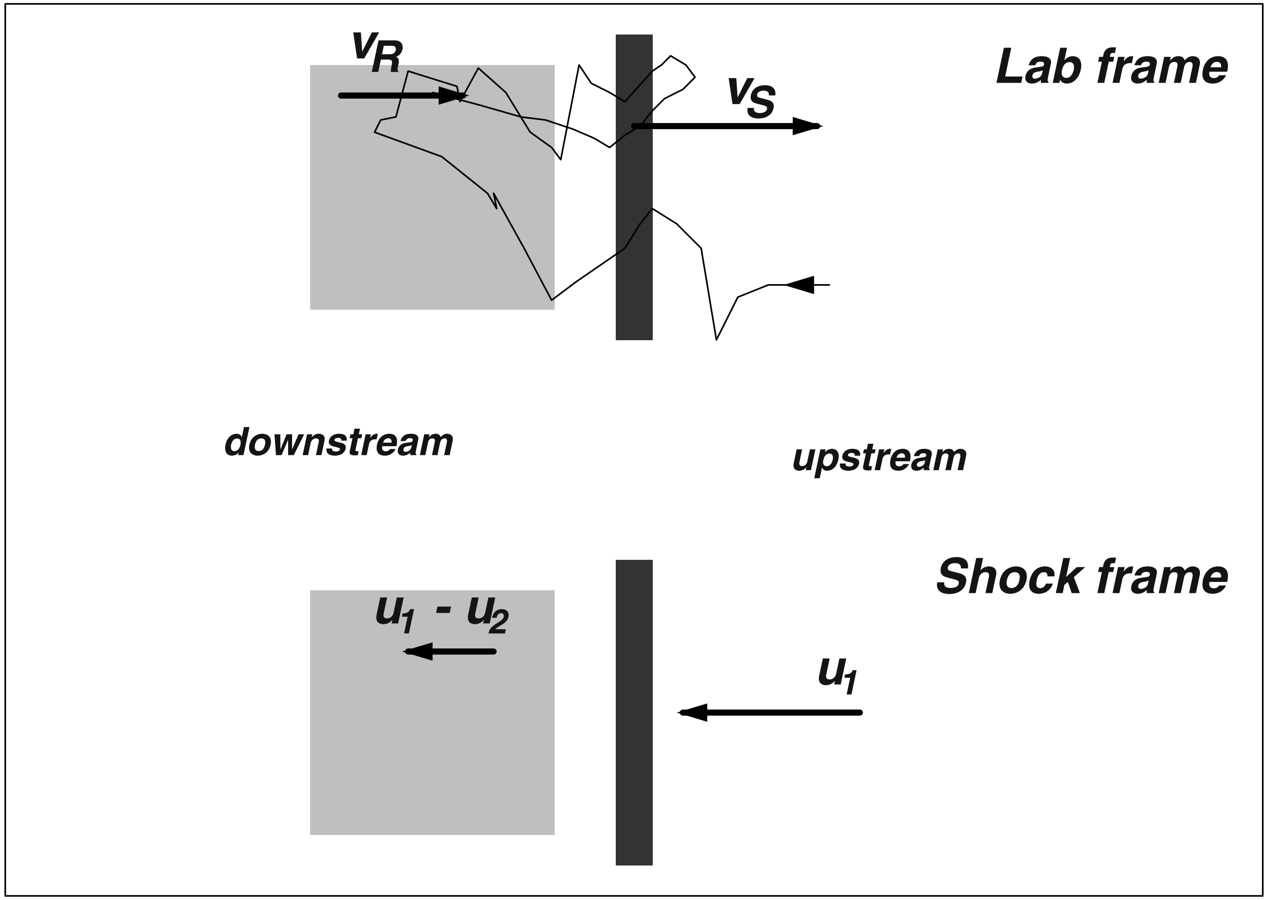

Fig. 3.9. Schematic representation of particle acceleration at astrophysical shocks. The upper panel shows the velocities and the motion of a test particle in the Lab frame. The lower panel shows the velocities in the shock frame.

shock acceleration

1st order Fermi acceleration

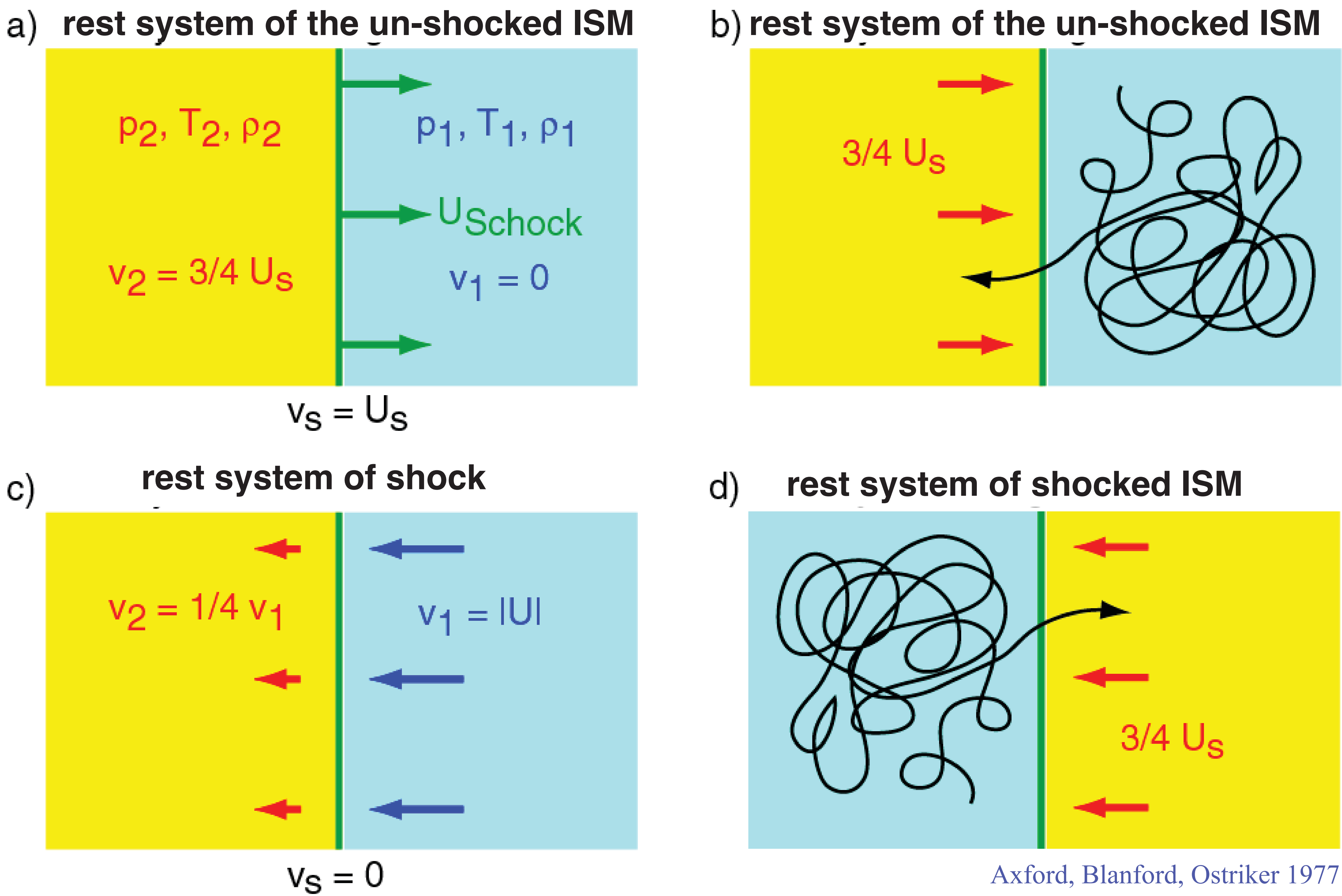

Axford, Blanford, Ostriker 1977 ff

acceleration mechanism:

1) particles in the ISM before the shock

2) shock front passes particles
plasma cloud moves $\frac{3}{4}U_s$

energy gain $\frac{\Delta E}{E} \propto \frac{U_s}{c}$

3) isotropized particles stay close to the shock and again move towards the shock front

--> energy gain $\frac{\Delta E}{E} \propto \frac{U_s}{c}$

4) going back to 2)

remarks:

1) fully symmetric before and after the shock

2) on average, only head-on collisions

3) process is very fast
particles stay in vicinity of shock front
and are accelerated at each encounter $\propto \frac{U_s}{c}$

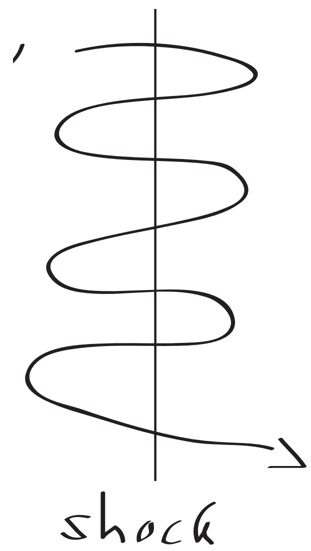

at some point the particles escape,
because their energy is too high to
be reflected by the B fields

Particle acceleration at astrophysical shocks

β^2 (second-order (Fermi) acceleration).

this mechanism is much faster than original Fermi acceleration
—> 1st order Fermi acceleration, proportional to β

Shock acceleration gives a definite prediction for the spectral index γ of the power law spectrum of the accelerated particles. For a large plane shock the rate of shock encounters is the projection of the isotropic cosmic ray flux of density ρ_{CR} onto the plane front of the shock, which is $c\rho_{CR}/4$. The rate of escaping the shock through convection downstream away (which is the only way of leaving a plane shock of infinite length) is the product of the same cosmic ray density times the convection velocity u_2. The escape probability is the ratio of the escape rate to the encounter rate

$$P_{esc} = \frac{\rho_{CR} u_2}{c\rho_{CR}/4} = \frac{4u_2}{c}.$$

1st order Fermi acceleration gives prediction for spectral index

$$\gamma = \frac{P_{esc}}{\xi} = \frac{4u_2}{c} \times \frac{3c}{4(u_1 - u_2)} = \frac{3}{u_1/u_2 - 1} \sim 1$$

SNR shock waves with v~10^9 cm/s and sound speed of ISM 10^6 cm/s

Particle acceleration at astrophysical shocks

maximum energy of shock acceleration

mean free path of magnetic scattering λ_S **> particle gyro radius** r_g.

energy gain limited by $$\frac{dE}{dt} \leq \frac{\xi E u_1}{r_g} = \frac{u_1}{c} ZeBu_1 \, .$$

The maximum energy that a charged particle could achieve is then expressed as a function of the shock velocity and extension and the value of the average magnetic field as

$$E_{max} = \frac{u_1}{c} ZeB(u_1 t) = \frac{u_1}{c} ZeBr_S. \qquad (E = pc)$$

Sources of Cosmic Rays

Galactic sources

Supernovae

We have seen already that Supernovae produce enough energy.
And shock fronts are observable at SNRs.

expansion velocity of shock front up to $20 - 30 \cdot 10^3 \ \frac{\mathrm{km}}{\mathrm{s}}$
(M>>1)

duration up to 100000 a
--> diameter of ~2-3 kpc

Kepler's supernova 1604, d ~ 8 kpc

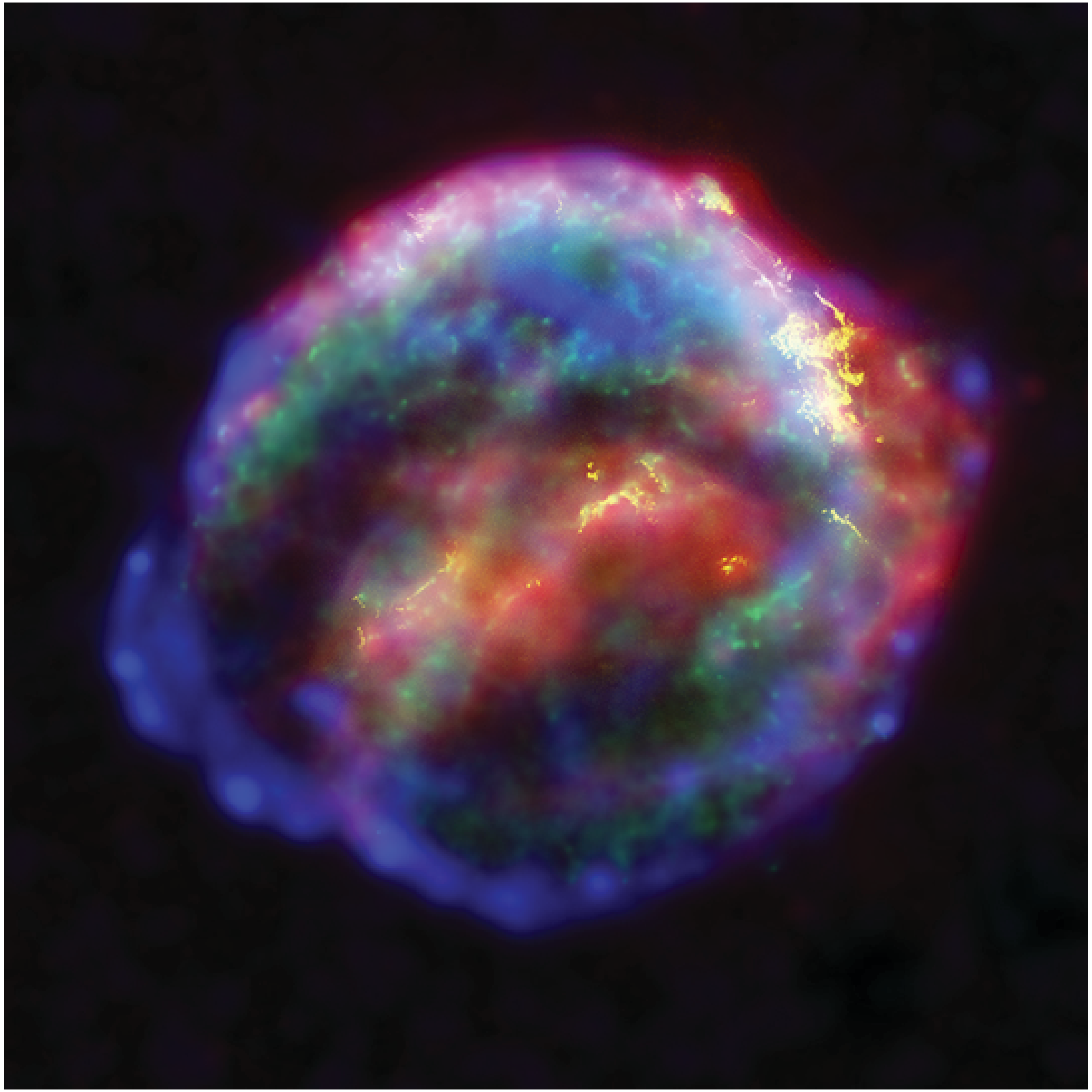

X-ray, Optical & Infrared Composite of Kepler's SNR

Tycho's supernova 1572, d ~ 2.3 kpc
$v_s \sim 4600 +/- 400$ km/s
$E_{kin} \sim 5*10^{50}$ erg

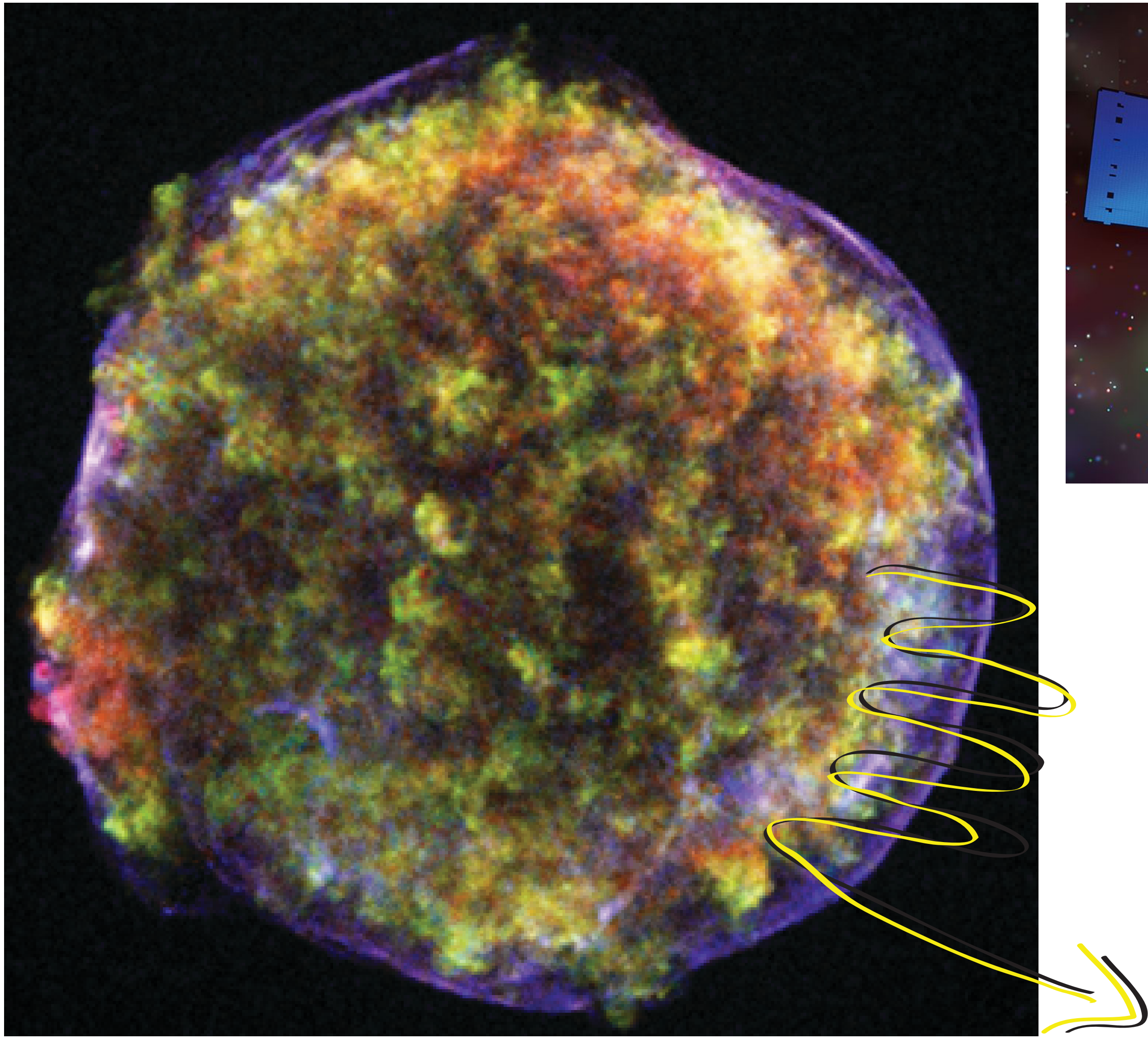

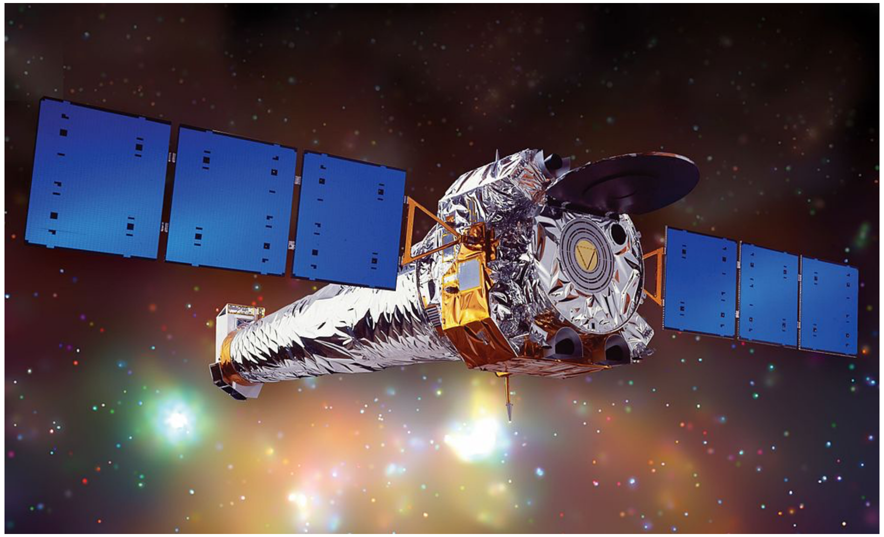

Chandra x-ray image

Particle acceleration at astrophysical shocks

maximum energy of shock acceleration

The maximum energy achievable at supernova remnants is estimated by Lagage & Cesarsky [58]. They show that most of particle acceleration happens before the shock has swept up mass equal to the mass of the ejecta, i.e. when the average density times the volume of the remnant equals the mass of the ejecta.

$$\frac{4}{3}\pi(u_1 t)^3 \rho_{IS} = M_{SR}. \tag{3.24}$$

For $M_{SR} = 10 M_\odot$ and $u_1 = 10^9$ cm/s and interstellar medium with density 1 nucleon per cm^3 the maximum energy is

$$\boxed{E_{max} = Z \times 2.4 \times 10^5 \text{ GeV}.} \tag{3.25}$$

The original number of Lagage & Cesarsky is 3×10^4 GeV since they use an expansion velocity of 5×10^8 cm/s. A higher value is derived for a lower value of the interstellar density. Some more detailed recent calculations [59] derive values close to 5×10^5 GeV.

SN 1006
x-ray image

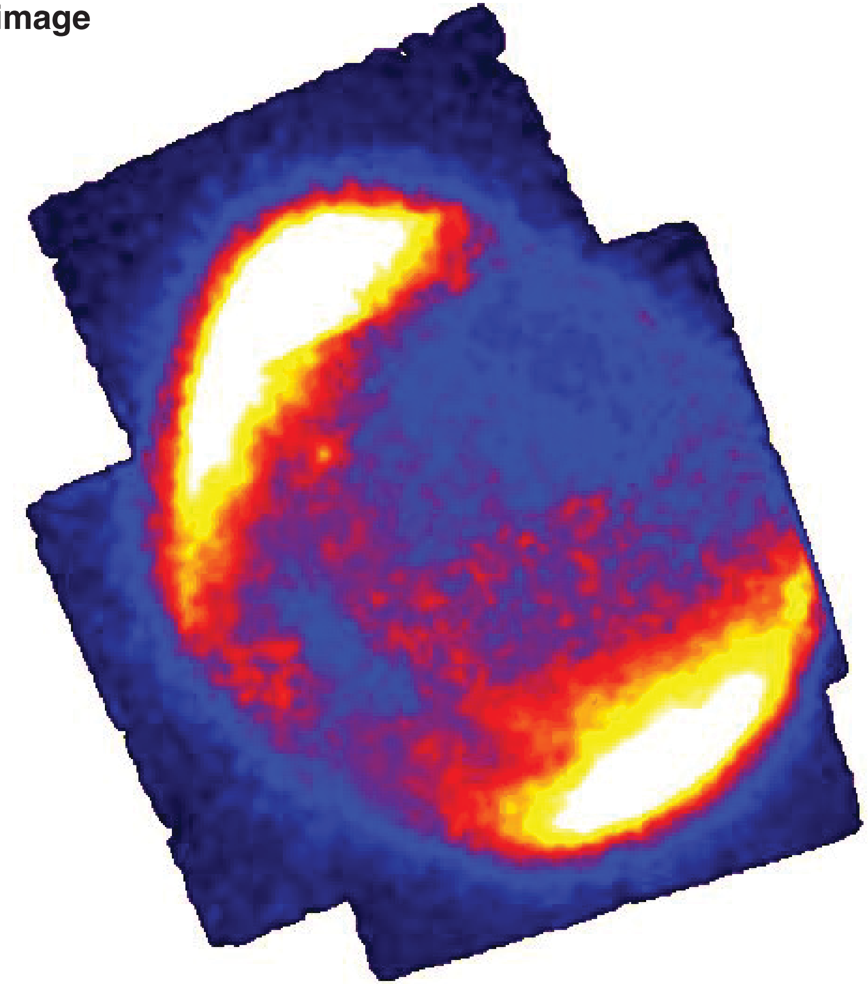

SNR measured in x-rays —> acceleration of particles (at least electrons)

ASCA (Advanced Satellite for Cosmology and Astrophysics)

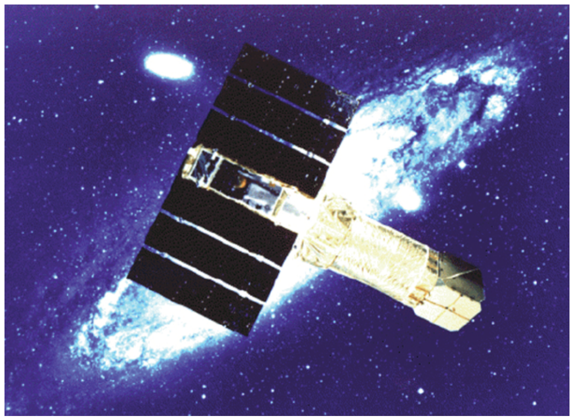

SN emits radiation in x-ray regime

(high plasma temperatures)

radio emission through synchrotron radiation of electrons

energy loss: $$-\frac{dE}{dt} \propto \left(\frac{E}{M_0}\right)^4 \propto \gamma^4$$ ***r* fixed**

$$-\frac{dE}{dt} \propto B^2\gamma^2$$ ***r* free**

--> important for electrons (10^4 compared to protons)

--> confirmation of shock acceleration of particles

(striclty speaking only for electrons)

H.E.S.S. supernova remnant RXJ 1713

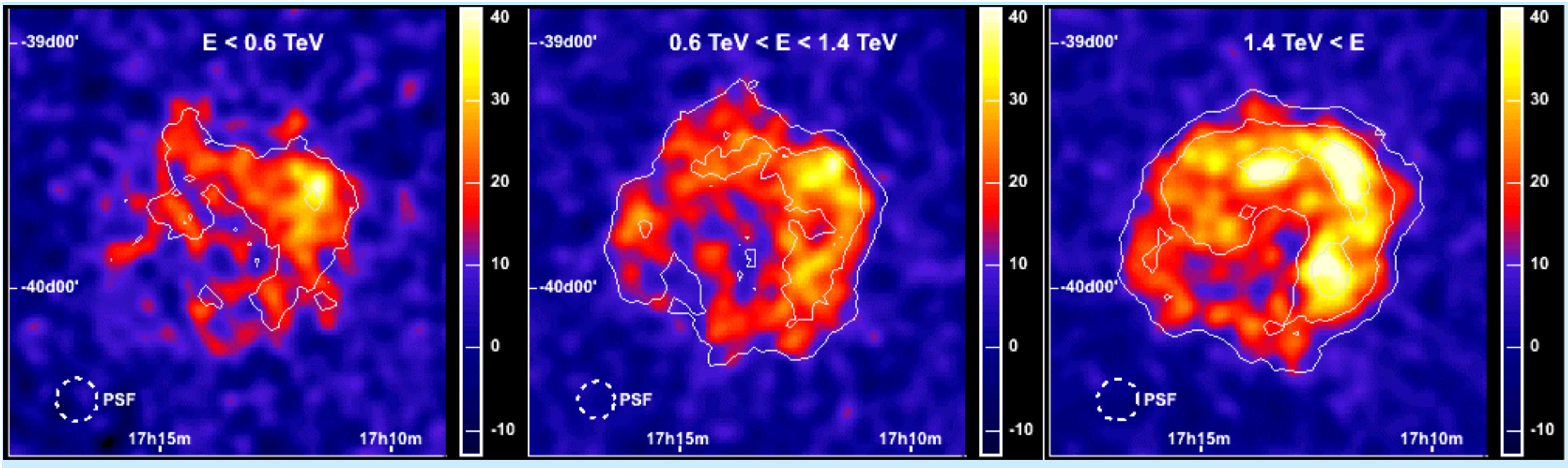

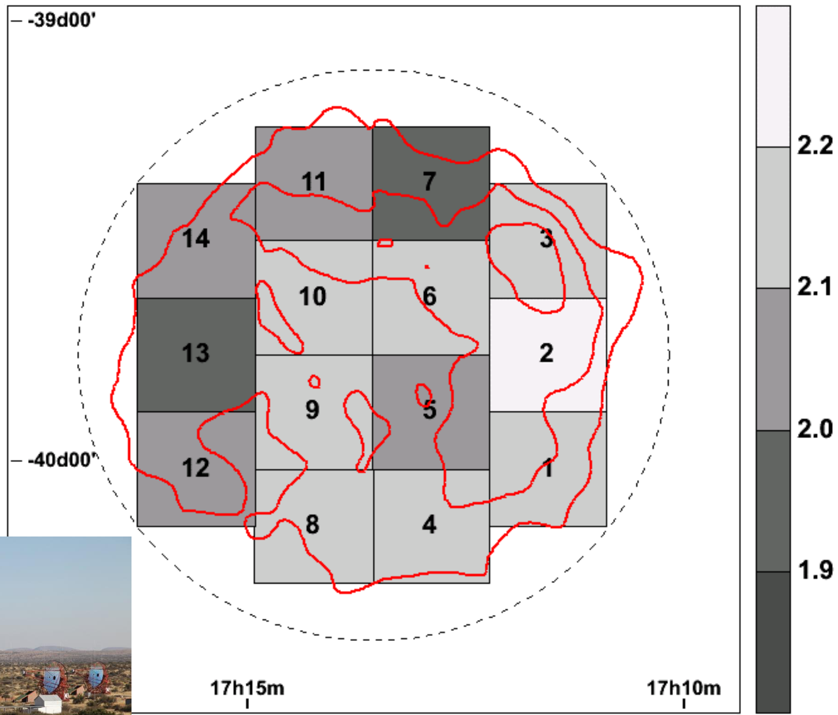

measured in TeV gamma rays

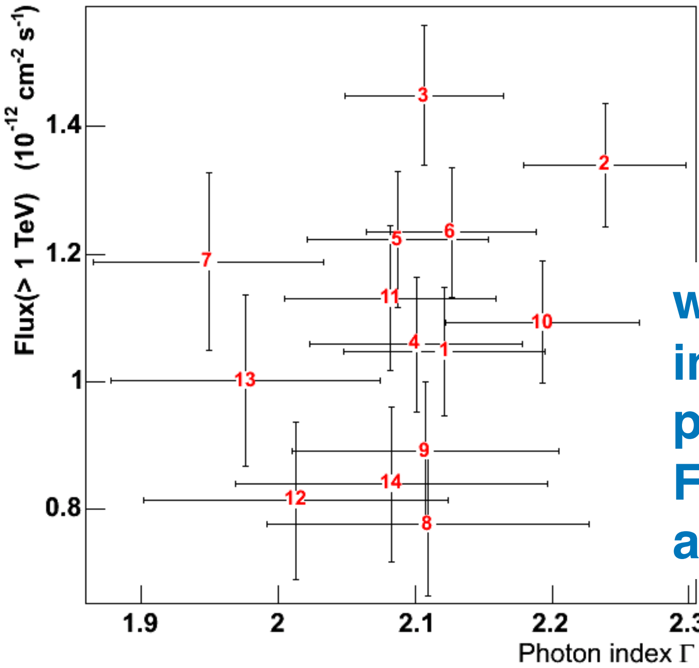

with spectral index as predicted by Fermi acceleration

Acceleration - additional considerations

so far we assumed that the B field is normal to the shock front (parallel shock)

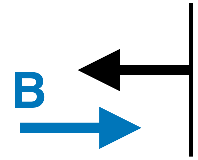

for perpendicular shock, acceleration is aided by electric field, created by inflow of magnetized plasma from the upstream region

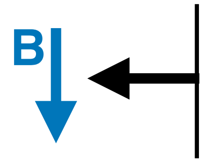

magnitude of electric field $E = u_1 \times B/c.$

Charged particles gain energy very fast when they move along the plane shock. The energy gain is proportional to the distance along the shock and to the electric field value – $\Delta E = ZeEl.$

—> effective energy gain, could be orders of magnitudes higher than in parallel shocks

Acceleration - additional considerations

Another important consideration is the possibility that the supernova remnant may evolve not in the typical interstellar medium, but rather in the hot and highly magnetized environment created by the stellar winds of the progenitor star [61]. Red giants, the typical supernova type II progenitors, have very heavy mass loss during the later stages of their evolution, possibly exceeding $10^{-7}\,M_\odot$ *per year. The surface magnetic field of the progenitor star is frozen into the stellar wind plasma. The medium in which at least some supernova remnants expand is much denser and has stronger magnetic fields than the typical interstellar medium. Völk & Biermann [61] use the example of the extreme Wolf–Rayet stars, where the maximum acceleration energy for protons could exceed* 10^{17} *eV.*

Wolf-Rayet star

acceleration seems to be feasible up to values exceeding E > Z*10^{17} eV